

Relaxation and magnetic reconnection in plasmas

J. B. Taylor

Culham Laboratory, Abingdon, Oxfordshire, OX14 3DB, England

The theory of plasma relaxation is described and developed. Turbulence, allied with a small resistivity, allows the plasma rapid access to a particular minimum-energy state. This process involves reconnection of magnetic field lines in a manner that destroys all the topological invariants of ideal plasma so that only total magnetic helicity survives. Although this mechanism, and the equations describing the relaxed state, are similar in all systems, the properties of the relaxed state depend crucially on the topology—toroidal or spherical—of the container and on the boundary conditions. Consequently there are several different types of relaxed state, each with its own special characteristics, which are derived and discussed. The measurements made on many experiments, including toroidal pinches, OHTE, multipinch, and spheromaks, are reviewed and shown to be in striking agreement with the theoretical predictions.

CONTENTS

I. Introduction	741
A. Background	741
B. Plasma relaxation	742
C. Additional comments on relaxation	743
D. Boundary conditions and the invariant	744
E. Plasma pressure	745
II. Relaxed State in a Large-Aspect-Ratio Torus	745
III. Further Properties of Relaxed States in a Large-Aspect-Ratio Torus	746
IV. General Toroidal Relaxed States	748
V. The Multipinch Experiment and Axisymmetric Relaxed States	748
VI. Relaxed States in Other Systems	751
A. Spheromak	751
1. Relaxed states of spheromak	752
2. Spheromak experiments	753
B. Flux-core spheromak (FCS)	754
1. Relative helicity	755
2. Relaxed states	756
3. Experiments	757
VII. Stability of Relaxed States	757
VIII. Summary and Conclusions	758
Acknowledgments	759
Appendix A: General Theory of Relaxed States	759
1. Toroidal systems	759
2. Spherical systems	760
Appendix B: Lowest-Energy State Versus μ	761
References	761

I. INTRODUCTION

A. Background

In this paper a plasma is regarded as a conducting fluid having small resistivity and small viscosity. Even in this simple model interaction of the plasma with magnetic fields leads to extremely complex behavior, especially when turbulence occurs. It is therefore remarkable that one can make *quantitative* predictions about the plasma configuration resulting from such turbulence. This is possible because the turbulence, allied with small resistivity, allows the plasma rapid access (in a time short com-

pared with the usual resistive diffusion time) to a particular minimum-energy state. This process, known as plasma relaxation, involves the reconnection of magnetic field lines and is a remarkable example of the self-organization of a plasma (Hasegawa, 1985). Since plasma turbulence occurs frequently, so does this relaxation process, and the theory has now been successfully applied to plasmas in many different laboratory systems (see references herein) and even to astrophysical plasmas (Heyvaerts and Priest, 1984; Konigl and Choudhuri, 1985).

An important concept in the theory is that of magnetic helicity, $\int \mathbf{A} \cdot \mathbf{B} d\tau$, as an invariant of plasma motion. This was used by Woltjer (1958) and by Wells and Norwood (1969), but relaxation theory as described here began with the work of Taylor (1974a, 1975, 1976), which explained why total helicity alone, rather than the infinity of invariants of ideal magnetohydrodynamics, should be important and determined the properties of the relaxed states of toroidal plasmas. These calculations showed that the relaxed state accounted quantitatively for many hitherto unexplained observations on toroidal pinch experiments.

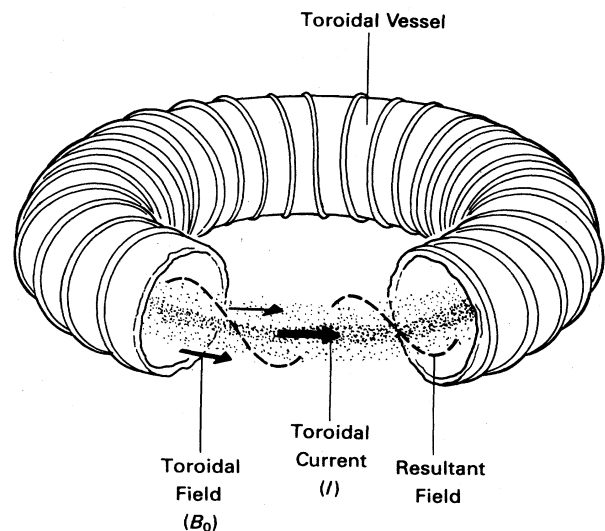


FIG. 1. The toroidal pinch.

TABLE I. Toroidal pinch experiments. Representative parameters. Based on a table prepared by Ortolani and Rostagni (1983), with additional data from Bodin and Newton (1980), Watt *et al.* (1985), and Toyama *et al.* (1985).

	ZETA	ALPHA	ETA-BETA	TPE-1R(M)	ZT-40(M)	OHTE	HBTX-1A	REPUTE
R (m)	1.50	1.60	0.65	0.5	1.14	1.24	0.8	0.82
a (m)	0.50	0.50	0.125	0.09	0.20	0.19	0.26	0.20
I (kA)	350		180	130	190	230	200	220
$I_{(\max)}$	900	300	280		440	500	500	260
T_e (eV)	200		40	300	150	75	50	
n (10^{20} m^{-3})			2	0.3	0.25	0.4	0.2	0.5

The toroidal pinch is one of the simplest systems for confining plasma by a magnetic field. In principle it involves only a toroidal vacuum vessel in which a toroidal magnetic field B_0 is first created by external coils (Fig. 1). Then, after creating an initial plasma by a suitable ionizing process, one induces a toroidal current I . This current heats and compresses the plasma through the well-known "pinch effect." [The principal parameters of several toroidal pinch experiments are shown in Table I. For details see, for example, the review by Bodin and Newton (1980).]

There are several remarkable features common to all toroidal pinch experiments. First, it is found that, after an initial highly turbulent phase, the plasma settles into a more quiescent state in which the fluctuations are reduced. Second, in this quiescent state the mean magnetic field profiles are essentially independent of the particular experiment or the previous history of the discharge and depend only on a single parameter, the pinch ratio $\theta \equiv 2I/aB_0$. Third, if θ exceeds a certain critical value the quiescent state is one in which the toroidal field is spontaneously reversed in the outer region of the plasma near the vessel wall [hence, the usual designation—reversed-field pinch (RFP)]. Typical mean magnetic field profiles are shown in Fig. 2.

It is clear from the behavior of plasma in the toroidal pinch that during the turbulent phase it seeks out a preferred configuration—the relaxed state. The idea of a re-

laxed state can be illustrated by a simple analogy. Suppose a flexible, current-carrying, closed loop of wire is immersed in a viscous medium; what configuration would it adopt when it is in equilibrium with its own magnetic field? So long as the wire is moving, energy is dissipated, so it will come to rest in a state of minimum energy subject to whatever constraints are applicable. If the wire is perfectly conducting, the magnetic constraint is that (LI) be constant (where L is the inductance), and if this were the only constraint the equilibrium, or relaxed state, would be found by minimizing $LI^2/2$ subject to this constraint. (This corresponds to a state of maximum inductance.)

B. Plasma relaxation

A plasma resembles an infinity of interlinked flexible conductors, and the problem is to identify the appropriate constraints. If there were no constraints the state of minimum energy would be a vacuum field with no plasma current. This is indeed the eventual state of an isolated resistive plasma, but is clearly not what we are concerned with here. At the other extreme, if the plasma is perfectly conducting, there is an infinity of constraints. These arise because the fluid moves precisely with the magnetic field, each field line maintains its identity, and the flux through any closed curve moving with the fluid is constant.

To express these constraints mathematically (Taylor, 1974a) we introduce the vector potential $\mathbf{B} = \nabla \times \mathbf{A}$. If the plasma is perfectly conducting, so that $\mathbf{E} + \mathbf{v} \times \mathbf{B} = 0$, the vector potential must satisfy

$$\frac{\partial \mathbf{A}}{\partial t} = \mathbf{v} \times \mathbf{B} + \nabla \chi. \quad (1.1)$$

Clearly any change in the component \mathbf{A} perpendicular to \mathbf{B} can be accommodated by a suitable choice of \mathbf{v} , so Eq. (1.1) imposes no constraint on changes of \mathbf{A}_\perp . However, despite the arbitrary gauge χ , there are constraints on A_\parallel , the component of \mathbf{A} parallel to \mathbf{B} . From Eq. (1.1) we have

$$\mathbf{B} \cdot \nabla \chi = \mathbf{B} \cdot \frac{\partial \mathbf{A}}{\partial t}. \quad (1.2)$$

This is a magnetic differential equation (Kruskal and Kulsrud, 1958) for χ which can be satisfied only if

$$\oint \frac{dl}{B} \left[\mathbf{B} \cdot \frac{\partial \mathbf{A}}{\partial t} \right] \text{ and } \oint \frac{dS}{|\nabla \psi|} \left[\mathbf{B} \cdot \frac{\partial \mathbf{A}}{\partial t} \right] \quad (1.3)$$

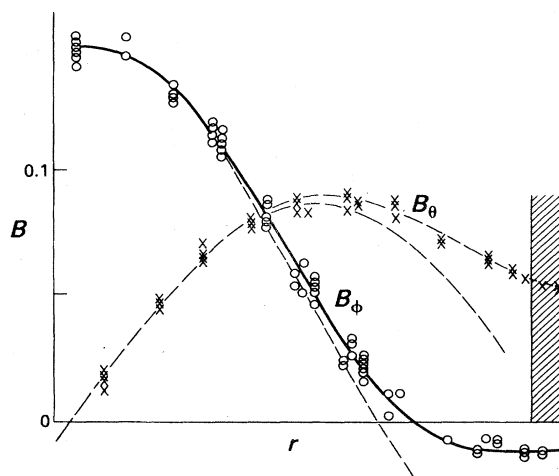


FIG. 2. Experimental and theoretical magnetic field profiles. HBTX-1A (from Bodin, 1984).

are zero on each closed field line and each magnetic surface, respectively. The variation A_{\parallel} must be constrained accordingly. A convenient way to express this constraint (Taylor, 1974a) is that for every infinitesimal flux tube surrounding a closed line of force the quantity

$$K(\alpha, \beta) = \int_{\alpha, \beta} \mathbf{A} \cdot \mathbf{B} d\tau \quad (1.4)$$

is an invariant. (Here α, β label the line of force.) This infinity of invariants replaces the single invariant (LI) of the flexible wire loop. Note that these invariants are essentially *topological*—they require the identification of lines of force and represent the linkage of lines of force with one another (Moffatt, 1978; Berger and Field, 1984). They state that if one closed field line initially links another n times then in a perfectly conducting plasma the two loops must remain linked n times during any subsequent plasma motion.

If we minimize the magnetic energy,

$$W = \frac{1}{2} \int (\nabla \times \mathbf{A})^2 d\tau \quad (1.5)$$

subject to the infinity of constraints described above, then for a plasma confined by a perfectly conducting toroidal shell we find that the equilibrium state satisfies

$$\nabla \times \mathbf{B} = \lambda(\alpha, \beta) \mathbf{B}, \quad (1.6a)$$

$$\mathbf{B} \cdot \nabla \lambda = 0. \quad (1.6b)$$

Thus the state of minimum magnetic energy when all the constraints of a perfectly conducting plasma are observed is some force-free equilibrium. (This is hardly surprising, since the plasma internal energy has been ignored.) However, this cannot be the appropriate description of the quiescent state, for in order to determine the Lagrange multiplier¹ $\lambda(\alpha, \beta)$ one would have to calculate the invariant $K(\alpha, \beta)$ for each closed field line and relate it to its initial value. Hence, far from being universal and independent of initial conditions, the state defined by Eq. (1.6) depends on every detail of the initial state.

To escape from this dilemma we must recognize that real plasmas, especially turbulent ones, are never perfectly conducting in the sense discussed above. In the presence of resistivity, however small, topological properties of lines of force are no longer preserved. Lines of force may break and reconnect even though the resistive diffusion time may be very long and there is insignificant flux dissipation. Mathematically the situation is one of nonuniform convergence; when $\eta = 0$ the equations do not permit changes in the topology of field lines, whereas such changes may occur when $\eta \neq 0$, even in the limit of small η . Physically, as $\eta \rightarrow 0$, the regions over which resistivity

acts get smaller, but the field gradients get correspondingly larger and the rate of reconnection does not diminish as fast as η and may not diminish at all. Furthermore, the effect of local reconnection is felt throughout the plasma. A similar process is involved in resistive instabilities (Furth *et al.*, 1963; Furth, 1985) and magnetic reconnection at X points (Parker, 1957; Sweet, 1958; Petschek, 1965; Vasyliunas, 1975; White, 1983).

We conclude that, in a turbulent resistive plasma, flux tubes have no continuous independent existence. Consequently all the topological invariants $K(\alpha, \beta)$ cease to be relevant, not because the magnetic flux changes significantly, but because it is no longer possible to identify the field line to which the flux belongs. However, the sum of all the invariants, that is the integral of $(\mathbf{A} \cdot \mathbf{B})$ over the total plasma volume V_0 , is independent of any topological considerations and of the need to identify field lines. Consequently, it remains a good invariant so long as the resistivity is small. An alternative description is that during turbulence the field lines become chaotic and all parts of the plasma are connected along any line of force. A model of flux tubes in a turbulent plasma closely related to this interpretation has been discussed by Rusbridge (1977, 1982).

To obtain the relaxed state of a slightly resistive turbulent plasma, therefore, we must minimize the energy subject to the single constraint that the total magnetic helicity

$$K_0 = \int_{V_0} \mathbf{A} \cdot \mathbf{B} d\tau \quad (1.7)$$

be invariant. For a plasma enclosed by a perfectly conducting toroidal shell (which incidentally ensures that the toroidal flux ψ is also invariant), the corresponding equilibrium satisfies

$$\nabla \times \mathbf{B} = \mu \mathbf{B}, \quad (1.8)$$

where μ is a constant. This relaxed state depends only on a single parameter μ —which is directly related to the pinch parameter $\theta = \mu a / 2$. Already, therefore, this reproduces one aspect of the quiescent state. We shall show later that the relaxed state is completely determined by the two invariants K_0 and ψ .

C. Additional comments on relaxation

Before discussing the nature of the relaxed states defined by Eq. (1.8), we offer some further remarks on the relaxation process that may be useful. During relaxation the plasma energy decays, while total helicity K_0 remains essentially constant. This difference in decay rates is a consequence of the turbulent fluctuations. In a nonturbulent plasma, helicity and energy both decay slowly on a resistive time scale

$$\dot{K} \sim -2\eta \int \mathbf{J} \cdot \mathbf{B} \quad \text{and} \quad \dot{W} \sim -\eta \int J^2, \quad (1.9)$$

but for small-scale fluctuations

¹Strictly, the minimization cannot be treated by a simple Lagrange multiplier, since the paths over which the constraints are applied themselves vary with $\delta \mathbf{A}$. An extension of the Lagrange multiplier technique is necessary, but the final result is indeed the elementary one of Eq. (1.6).

$$\dot{K} \sim -2\eta \sum k B_k^2 \quad \text{and} \quad \dot{W} \sim -\eta \sum k^2 B_k^2, \quad (1.10)$$

so that energy dissipation is finite at scale lengths $k \sim \eta^{-1/2}$, whereas helicity dissipation is only $\sim \eta^{1/2}$ at this scale. (One may also note that viscosity dissipates turbulent energy but has no direct effect on helicity.) The generation of small-scale turbulence is related to field line reconnection through the condition $\mathbf{B} \cdot \nabla \lambda = 0$ for a stationary force-free plasma (i.e., λ must be uniform along a field line). When two field lines having different values of λ connect, the subsequent adjustment of λ is brought about by small-scale (Alfvén wave) motion. Thus relaxation inherently requires both large- and small-scale fluctuations.

There have been several attempts at computer simulation of the relaxation process (Sykes and Wesson, 1977; Riyopoulos *et al.*, 1982; Caramana *et al.*, 1983; Aydemir and Barnes, 1984; Aydemir *et al.*, 1985; Sato and Kusano, 1985). These simulations lend some support to the picture described above, but because of the inherent difficulties of simulating large-Reynolds-number turbulence a conclusive demonstration of the detailed mechanism (and hence of the time scale for relaxation) has not yet been given. In this connection it must be emphasized that relaxation is fundamentally a three-dimensional process. In some simulations (e.g., Caramana *et al.*, 1983) the motion is restricted to a two-dimensional helically symmetric form.² In this event the imposed symmetry introduces, in addition to K_0 , an infinity of additional constraints (Bhattacharjee *et al.*, 1980; Bhattacharjee and Dewar, 1982)

$$K_\alpha = \int \chi^\alpha (\mathbf{A} \cdot \mathbf{B}) d\tau \quad (1.11)$$

(where χ is the helical flux), which are not present in fully three-dimensional turbulence. Indeed, an interesting mathematical viewpoint (Hameiri and Hammer, 1982) of the central role played by K_0 is that it is the only member of the set K_α that is independent of the pitch of the assumed helical symmetry, and therefore is the only one that persists when disturbances of all pitch lengths are present.

D. Boundary conditions and the invariant

A comment is also necessary on the nature of the boundary conditions that are assumed during relaxation. At a perfectly conducting boundary, the normal component B_n of the magnetic field is fixed, and for the present we consider only $B_n = 0$. One consequence of the boundary condition is that the toroidal flux ψ in the plasma is invariant. In terms of the vector potential \mathbf{A} the boundary conditions in a toroidal system require that $\oint \mathbf{A} \cdot d\mathbf{l}$ and $\oint \mathbf{A} \cdot d\mathbf{s}$ (where $\oint d\mathbf{l}$ and $\oint d\mathbf{s}$ denote loop integrals

along closed paths the long and short way around the toroidal boundary) should be fixed. In this case $\oint \mathbf{A} \cdot d\mathbf{s}$ prescribes the toroidal flux ψ .

Some additional features of the invariant K_0 should also be noted. One of these concerns gauge invariance. Under a gauge transformation $\mathbf{A} \rightarrow \mathbf{A} + \nabla \chi$ the change in the helicity K_0 is

$$\int \mathbf{B} \cdot \nabla \chi d\tau = \oint \chi \mathbf{B} \cdot d\mathbf{S}. \quad (1.12)$$

With the boundary condition $\mathbf{B} \cdot \mathbf{n} = 0$ the surface integral vanishes and K_0 is indeed gauge invariant. Nevertheless, difficulties may arise because the interior of the torus is a multiply connected region in which χ may not be single valued. To overcome this it is sometimes convenient (Bevir and Gray, 1980; Taylor, 1980) to replace K_0 by

$$K_1 = \int \mathbf{A} \cdot \mathbf{B} d\tau - \oint \mathbf{A} \cdot d\mathbf{l} \oint \mathbf{A} \cdot d\mathbf{s}, \quad (1.13)$$

where $d\mathbf{l}$ and $d\mathbf{s}$ again denote loop integrals the long and short way around the toroidal surface. If a complete conducting shell surrounds the plasma, these loop integrals are constant, and nothing in our discussion is changed; K_1 is invariant during relaxation just as K_0 is. The advantage of Eq. (1.13) is that it is manifestly gauge invariant, even for multivalued gauge potentials.

If the boundary of the plasma is not a flux surface (i.e., $B_n \neq 0$ everywhere on the boundary), then (1.12) is nonzero and the helicity is not well defined. This reflects the fact that $(\mathbf{A} \cdot \mathbf{B})$ is not a local quantity. One cannot specify the "local" helicity at a point—only the total helicity within a flux surface. Where the helicity is located within that surface is not a valid question, any more than is the related question of where the linkage between two interlinked hoops is located. Consequently the question of gauge invariance and the definition of helicity must be reconsidered when we discuss systems in which $B_n \neq 0$ on the boundary (see Sec. VI.B).

Although the helicity K_1 is invariant when the plasma is enclosed within a complete conducting shell, it does change when an external loop voltage V_l is applied across a gap in the toroidal shell (as when the toroidal discharge is first created). According to Eq. (1.13) this change can be expressed as

$$\frac{dK_1}{dt} = 2V_l \psi, \quad (1.14)$$

where ψ is the toroidal flux. This shows that helicity can be given a practical interpretation (Taylor, 1975); at constant toroidal flux it is proportional to the volt-seconds stored in the discharge. Equation (1.14) also shows that by suitably phased simultaneous oscillation of V_l and ψ helicity can be continuously fed into the plasma without the need for a continuous supply of volt-seconds (Bevir and Gray, 1980). The mean rate of helicity injection is

$$\left\langle \frac{dK_0}{dt} \right\rangle = \left\langle \frac{dK_1}{dt} \right\rangle = 2 \langle \tilde{V} \tilde{\psi} \rangle. \quad (1.15)$$

²These are referred to as "single-helicity" computations. The term "helicity" in this context should not be confused with its meaning elsewhere in this paper.

E. Plasma pressure

A comment is also necessary on the role of the plasma pressure. Relaxation proceeds by reconnection of lines of force, and during this reconnection plasma pressure can equalize itself so that the fully relaxed state is also a state of uniform pressure. Hence, the inclusion of plasma pressure does not change our conclusions about the relaxed state. Of course, one may argue that pressure relaxation might be slower than field relaxation, so that the former was incomplete and some pressure gradients would remain. A pressure gradient can be introduced directly (Kondoh, 1981; Edenstrasse and Schuurman, 1983) or by incorporating additional invariants (Bhattacharjee *et al.*, 1980; Turner and Christiansen, 1981; Bhattacharjee and Dewar, 1982). However, no convincing argument for determining the correct residual pressure gradient has yet been given. We shall, therefore, consider ∇p to be negligible in relaxed states—which in any event is a good approximation for low- β plasmas.

II. RELAXED STATE IN A LARGE-ASPECT-RATIO TORUS

We now return to the properties of the relaxed state defined by Eq. (1.8). For a circular-cross-section torus of large-aspect ratio we may take the cylindrical limit in which the solution to Eq. (1.8) is

$$B_r = 0, \quad B_\theta = \alpha J_1(\mu r), \quad B_z = \alpha J_0(\mu r). \quad (2.1)$$

This is the well-known ‘‘Bessel function’’ solution. By straightforward calculation, μa (where a is the minor radius of the discharge) can be expressed as a function of K/ψ^2 (Martin and Taylor, 1974):

$$\frac{K}{\psi^2} = \frac{l}{2\pi a} \left[\frac{\mu a [J_0^2(\mu a) + J_1^2(\mu a)] - 2J_0(\mu a)J_1(\mu a)}{J_1^2(\mu a)} \right], \quad (2.2)$$

where l is the length of the cylinder—to be identified with $2\pi R$ in a toroidal system.

Thus the field profiles in the relaxed state are determined by K/ψ^2 , although as we have remarked earlier it is customary to label the relaxed states by the pinch ratio $\theta (= \mu a/2)$. In this regard one should note that although θ , μa , and K/ψ^2 are equally valid parameters for the final relaxed state, only K/ψ^2 is constant *during* relaxation. Note also that the relaxed state is completely determined by the two invariants K and ψ ; the ratio K/ψ^2 fixes the field profile, and either K or ψ then fixes the magnitude of the fields. No arbitrary or adjusted parameters are required in the theory.

The field profiles given by Eq. (2.1) agree well with those observed in the quiescent phase of many toroidal discharges. Figure 2 shows a comparison with measurements on HBTX-1A (Bodin, 1984). The other toroidal pinch experiments listed in Table I show similar profiles.

The onset of the spontaneous reversed toroidal field at

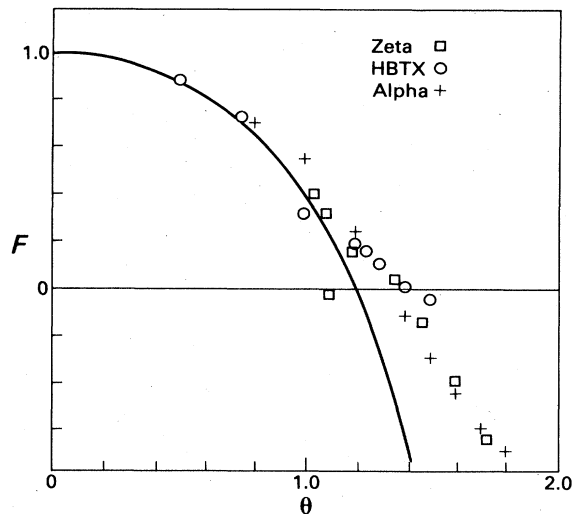


FIG. 3. F - θ diagram. Data from HBTX1, ALPHA, and ZETA and theoretical curve (from Bodin and Newton, 1980).

the wall can also now be determined. It occurs when $\mu a > 2.4$, i.e., when the pinch ratio $\theta > 1.2$. This result is also in good agreement with many observations. The relevant experimental data are usually presented through an F - θ diagram, where F is the ratio of toroidal field at the wall to the average toroidal field ($F < 0$ implies reversal). Figure 3 shows points on the F - θ curve for several experiments (Bodin and Newton, 1980), together with the corresponding theoretical curve. It is noteworthy that the experimental points in Fig. 3 do indeed all lie on a universal F - θ curve close to the theoretical curve, although the experimental value of θ for field reversal is somewhat higher than the theoretical value.

One reason for this discrepancy is that $\mu \equiv (\mathbf{j} \cdot \mathbf{B})/B^2$, which would be uniform in a fully relaxed state, falls off near the wall. The observed profile of $\mu(r)$ in the OHTE experiment (Ohkawa *et al.*, 1980; Tamano *et al.*, 1983) is shown in Fig. 4. Similar profiles have been observed in the ETA-BETA (Antoni *et al.*, 1983) and HBTX experiments (Bodin, 1984), and the effect of the $\mu(r)$ profile on

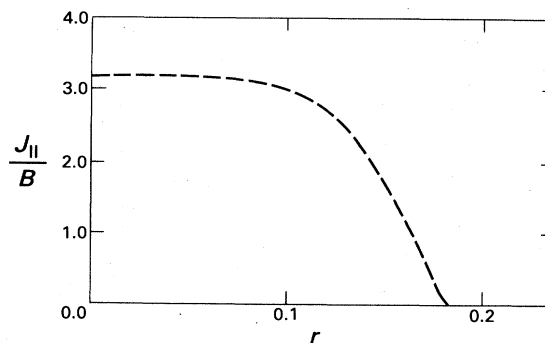


FIG. 4. Measured profile of $\mu(r)$. OHTE (from Tamano *et al.*, 1983).

the value of θ has been discussed in detail by Ortolani (1984). The fall in μ near the wall is believed to be due to the high plasma resistivity there—which the relaxation process cannot fully overcome.

Another reason for the discrepancy between the theoretical and experimental values of θ is that the measurements are often distorted by the flux-conserving liner and by toroidal plasma shifts. In recent experiments where θ is corrected for these effects, the agreement between theory and experiment is further improved (Newton, 1985).

Even more striking evidence for relaxation is observed in the time-dependent behavior of toroidal pinches. This is illustrated in the F - θ curves shown in Figs. 5 and 6. Figure 5(a) (Bodin and Newton, 1980) shows that during a fast current rise in HBTX the discharge is temporarily forced away from the relaxed state but quickly falls back to it and subsequently closely follows the theoretical F - θ curve. When the current rise is slower, the discharge lies close to the theoretical curve throughout [Fig. 5(b)]. Similar F - θ curves for ZT-40 (DiMarco, 1983), for OHTE (Tamaru *et al.*, 1979), and for REPUTE (Toyama *et al.*, 1985) are shown in Fig. 6.

These results, and many others from the experiments listed in Table I, show that the theory presented here accounts extremely well for the features of toroidal discharges described in the Introduction. We now turn to some additional and unexpected consequences of the theory.

III. FURTHER PROPERTIES OF RELAXED STATES IN A LARGE-ASPECT-RATIO TORUS

Determination of the relaxed state is actually more complex than we have indicated so far. This is because Eq. (1.8) may have several solutions compatible with the boundary conditions and with the given values of K and ψ . In this event, one must select that solution which has the lowest energy. The procedure can be demonstrated by considering again the large-aspect-ratio circular plasma (Taylor, 1975).

The general solution of Eq. (1.8) can be written (Chandrasekhar and Kendall, 1957) as

$$\mathbf{B} = \sum a_{mk} \mathbf{B}^{mk}(\mathbf{r}), \quad (3.1)$$

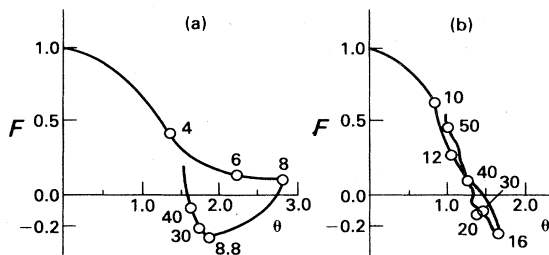


FIG. 5. Time-dependent F - θ curve for HBTX1. Times in μsec : (a) Fast mode; (b) slow mode (from Bodin and Newton, 1980).

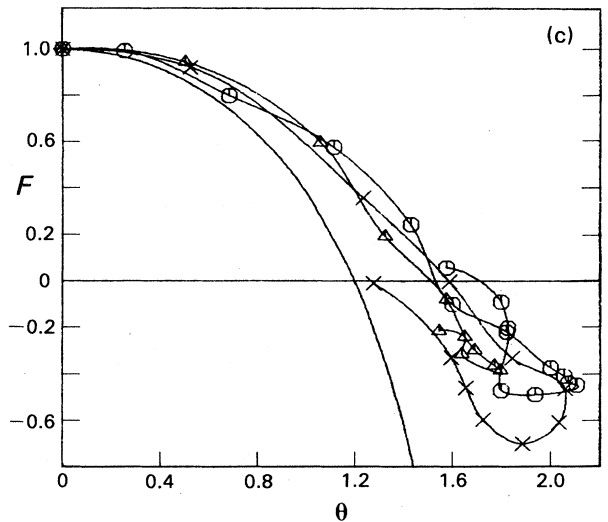
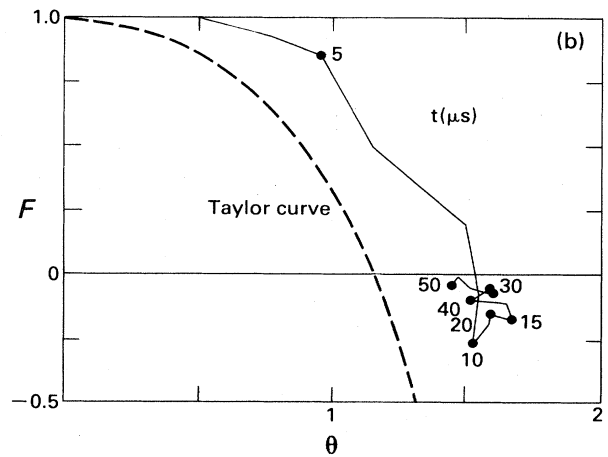
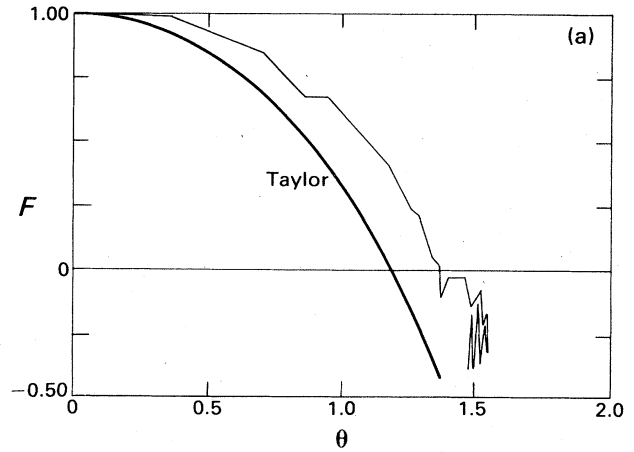


FIG. 6. Time-dependent F - θ curves: (a) ZT-40 experiment (from DiMarco, 1983); (b) TPRE experiment (from Tamaru *et al.*, 1979); (c) REPUTE experiment (from Toyama *et al.*, 1985).

where the a_{mk} are arbitrary and the individual \mathbf{B}^{mk} are

$$\begin{aligned}
 B_r^{mk} &= \frac{-1}{(\mu^2 - k^2)^{1/2}} \left[kJ'_m(y) + \frac{m\mu}{y} J_m(y) \right] \sin(m\theta + kz), \\
 B_\theta^{mk} &= \frac{-1}{(\mu^2 - k^2)^{1/2}} \left[\mu J'_m(y) + \frac{mk}{y} J_m(y) \right] \cos(m\theta + kz), \\
 B_z^{mk} &= J_m(y) \cos(m\theta + kz),
 \end{aligned}
 \tag{3.2}$$

with $y = r(\mu^2 - k^2)^{1/2}$.

Although this solution satisfies Eq. (1.8), we have not yet imposed the boundary condition $B_r(r=a)=0$, nor have we considered the value of the invariant K or the toroidal flux ψ . Before doing so, we should note an important feature of the above expressions, namely, that the $m=0, k=0$ term is different in character from all the others. This term satisfies the boundary condition for any value of μ and carries a nonzero toroidal flux. All the other terms satisfy the boundary condition *only* for discrete values of μ given by

$$\begin{aligned}
 ka [(\mu^2 - k^2)^{1/2} a] J'_m [(\mu^2 - k^2)^{1/2} a] \\
 + m\mu a J_m [(\mu^2 - k^2)^{1/2} a] = 0,
 \end{aligned}
 \tag{3.3}$$

and do not contribute any toroidal flux.

Thus, there are two distinct types of solutions to Eq. (1.8) which could satisfy the boundary conditions and correspond to the given toroidal flux. They are the following.

(i) The "symmetric" $m=0, k=0$ solution, which exists for any μ . For such a solution, as already noted, the appropriate value of μ is determined by the value of K/ψ^2 .

(ii) A "mixed" solution containing the $m=0, k=0$ term (to give the required toroidal flux) together with one of the other terms, i.e., a solution $(\alpha_0 \mathbf{B}^{00} + \alpha_{mk} \mathbf{B}^{mk})$. This mixed solution exists only for fixed discrete values of μ , and the role of the invariant K/ψ^2 is no longer to determine μ ; instead it determines the ratio α_{mk}/α_0 .

We see that both types of solutions are completely defined by the two invariants K and ψ , but in a different way in the two cases. We now need to determine which solution has the lowest energy. [Note there is only one solution of type (i), but there are many of type (ii).] It can be shown that the lowest-energy solution of Eq. (1.8) is that with the smallest μ (see Appendix B), so of all possible solutions of the second type, only that corresponding to the smallest root of Eq. (3.3) can be of interest. This smallest root occurs for $m=1, ka \approx 1.25$, and is given by $\mu a = 3.11$ (Martin and Taylor, 1974; see also Gibson and Whiteman, 1968).

The selection of the appropriate solution can now be made. The first "symmetric" solution is the lowest-energy state for all values of K/ψ^2 that correspond to $\mu a < 3.11$. For any larger value of K/ψ^2 the lowest-energy state is a "mixed" solution, with $\mu a = 3.11$ ($\theta \sim 1.6$) containing a helical component with $m=1$ and $ka \approx 1.25$. Since, for fixed toroidal flux, K/ψ^2 is proportional to volt-seconds in the discharge, the helical relaxed state arises when the volt-seconds exceed a critical value.

Furthermore, in the helical relaxed state, θ is independent of K/ψ^2 ; hence the plasma current (at fixed toroidal flux) does not increase with volt-seconds. The physical explanation for this is that above the critical value of K/ψ^2 the current channel becomes increasingly helically deformed as K/ψ^2 increases, and the increased inductive voltage absorbs the added volt-seconds. (In this regime, but not in the others, the plasma begins to resemble a single current filament, which seeks out a configuration of maximum inductance.) The amplitude of the helical deformation α_1/α_0 is given by (Martin and Taylor, 1974; Reiman, 1980)

$$\frac{K}{\psi^2} = \frac{l}{2\pi a} \left[8.21 + 4.49 \frac{\alpha_1^2}{\alpha_0^2} \right].
 \tag{3.4}$$

Thus we see that the theory of relaxed states predicts not one, but two, critical values of θ for the toroidal discharge (Taylor, 1975). At $\theta=1.2$ a reversed field is first generated, and at $\theta=1.6$ current saturation sets in. Evidence for this second critical θ was found in HBTX-1A (Butt *et al.*, 1975; Verhage *et al.*, 1978; Bodin and Newton, 1980) and is illustrated in Fig. 7. This shows a discharge in which θ was initially driven to a large value but quickly dropped back to around 1.6 and remained there for the rest of the discharge. The drop in θ was accompanied by the appearance of an $m=1$ helical distortion.

Not all toroidal pinches show a clear current limitation at $\theta \sim 1.6$, but when θ significantly exceeds this value there are usually increased fluctuations and a higher plas-

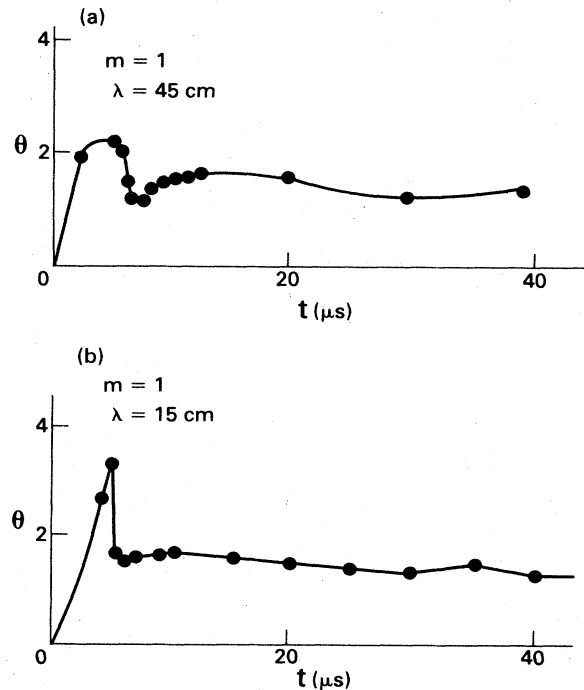


FIG. 7. Limitation of θ . HBTX1 (from Bodin and Newton, 1980).

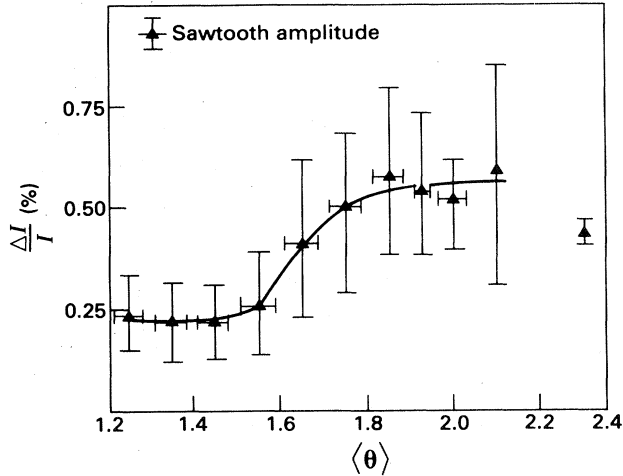


FIG. 8. Fluctuation level vs θ . ZT-40 (from Watt and Nebel, 1983).

ma resistance—indicating that the plasma is not fully relaxed. An example of this is shown in Fig. 8 (Watt and Nebel, 1983). We shall later describe much clearer evidence for current limitations (Sec. V). First, however, we must say something more about relaxed states in general toroidal systems.

IV. GENERAL TOROIDAL RELAXED STATES

The general theory of toroidal relaxed states follows closely that for the large-aspect-ratio circular pinch (Faber *et al.*, 1982,1985; Jensen and Chu, 1984) and is described in Appendix A. The present section is a summary of those features needed for the discussion of the multipinch experiment below, and is restricted to axisymmetric systems.

In general the relaxed state of a toroidal system is the lowest-energy solution of

$$\nabla \times \nabla \times \mathbf{A} = \mu \nabla \times \mathbf{A}, \quad (4.1)$$

with $\mathbf{n} \cdot \nabla \times \mathbf{A} = 0$ on the boundary and with $\oint \mathbf{A} \cdot d\mathbf{s}$, $\oint \mathbf{A} \cdot d\mathbf{l}$, and the helicity K given. In order to describe the relevant solutions we need also to consider the associated eigenvalue problem

$$\nabla \times \nabla \times \mathbf{a}_i = \lambda_i \nabla \times \mathbf{a}_i \quad (4.2)$$

with boundary condition $\mathbf{a}_i = 0$. (Note that because of this boundary condition an eigenfunction carries no toroidal flux.)

As in the circular case there can be many solutions of Eq. (4.1) that satisfy the boundary conditions and have the correct values of the invariants K and ψ ($= \oint \mathbf{A} \cdot d\mathbf{s}$), but only two of them are possible lowest-energy solutions. The first is an axisymmetric solution, analogous to the $m=0$, $k=0$ solution in the circular discharge. This may exist for any value of μ (except $\mu = \lambda_i$), and μ is determined by K/ψ^2 . The second is a superposition of the

first solution and the lowest eigenfunction (i.e., the eigenfunction with smallest eigenvalue³ λ_0). In this mixed solution, $\mu = \lambda_0$, and K/ψ^2 determines the amplitude of the eigenfunction component.

Bearing in mind that the lowest-energy solution is that with the smallest μ , we see that the first solution describes the relaxed state when K/ψ^2 is small and the corresponding μ is less than λ_0 . The second solution describes the relaxed state for larger K/ψ^2 , when $\mu > \lambda_0$ in the first solution. In this event the toroidal current (at fixed toroidal flux) is fixed and does not increase with K/ψ^2 . (Strictly, this second solution arises only if the lowest eigenfunction is “decoupled,” in the sense defined in Appendix A, but this is usually the case in axisymmetric systems. If the lowest eigenfunction is not decoupled, only the first type of solution is relevant. However, in this event $K/\psi^2 \rightarrow \infty$ as $\mu \rightarrow \lambda_0$, so that it is still true that μ can never exceed the smallest eigenvalue and that current saturation occurs at this point.)

Although the relaxed states of general axisymmetric systems are similar to those in the large-aspect circular-cross-section system, there is one important feature of the general system that is not apparent in the circular example. In that example the lowest eigenvalue ($\mu a = 3.11$) corresponds to a nonaxisymmetric eigenfunction, in fact to a helical mode with $m=1$, $ka=1.25$. [The lowest axisymmetric ($k=0$) eigenvalue is $\mu a = 3.83$ and is degenerate.] However, in a system with a highly convoluted cross section, the lowest eigenfunction may be axisymmetric. This is the case for the configuration of the “multipinch” experiment discussed in the next section and, as we shall see, it has important consequences.

V. THE MULTIPINCH EXPERIMENT AND AXISYMMETRIC RELAXED STATES

The multipinch, investigated at GA Technologies (La Haye *et al.*, 1984,1986), is an example of an axisymmetric toroidal system with noncircular cross section. The cross section resembles a figure eight whose height is about 2.5 times its width (Fig. 9). The major radius is 52.5 cm, the height 50 cm, and the width 20 cm. These dimensions were chosen so that the multipinch resembles two circular-cross-section pinches, similar to TPE-1R(M), one above the other. The method of operation of the multipinch is similar to that of other toroidal pinch experiments.

The axisymmetric relaxed states of the multipinch are readily found. An axisymmetric field can be written, in cylindrical coordinates R , φ , Z , as

$$\mathbf{B} = \frac{\mathbf{e}_\varphi \times \nabla \chi}{R} + \frac{\mathbf{e}_\varphi f}{R}. \quad (5.1)$$

³For systems with mirror symmetry the eigenvalues occur in pairs $\pm \lambda_i$. Otherwise one must consider separately states with positive and negative helicity.

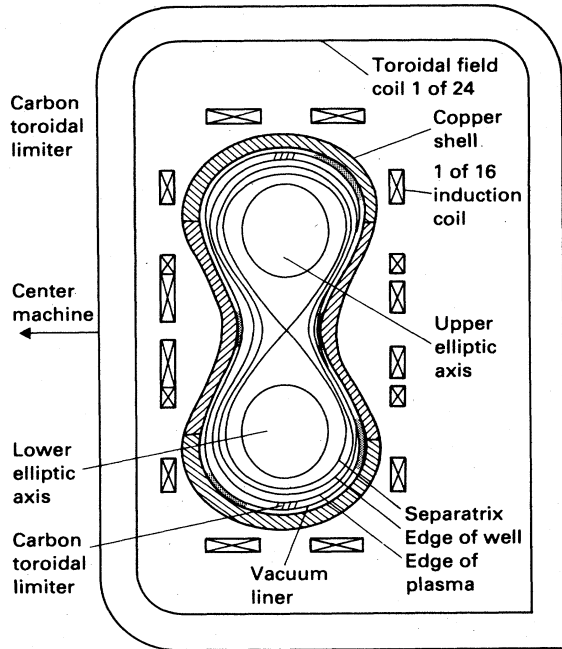


FIG. 9. Multipinch experiment (from La Haye *et al.*, 1986).

Then, for the relaxed state, Eq. (4.1) gives

$$\Delta^+\chi \equiv \frac{\partial^2\chi}{\partial z^2} + R \frac{\partial}{\partial R} \left[\frac{1}{R} \frac{\partial\chi}{\partial R} \right] = \mu f \quad (5.2)$$

and

$$\nabla f = -\mu \nabla \chi, \quad (5.3)$$

so that $f = C - \mu\chi$.

The boundary condition is $\chi = \text{const}$, and without loss of generality this constant can be set to zero. The toroidal flux condition then gives

$$\Psi = -\mu \int \frac{\chi}{R} dR dZ + C \int \frac{1}{R} dR dZ, \quad (5.4)$$

so, defining a toroidally weighted average,

$$\langle \rangle \equiv \left[\int \dots \frac{1}{R} dR dZ \right] \left[\int \frac{1}{R} dR dZ \right]^{-1}, \quad (5.5)$$

the equation for axisymmetric relaxed states becomes (La Haye *et al.*, 1986)

$$\Delta^+\chi + \mu^2\chi - \mu^2\langle\chi\rangle = \frac{\mu\langle R \rangle\Psi}{A}, \quad (5.6)$$

where A is the cross-section area of the discharge.

The corresponding axisymmetric eigenvalue problem, Eq. (4.2), becomes

$$\Delta^+\chi_i + \lambda_i^2(\chi_i - \langle\chi_i\rangle) = 0 \quad (5.7)$$

with $\chi_i = 0$ on the boundary.

Solutions of Eq. (5.6) can easily be computed, and an

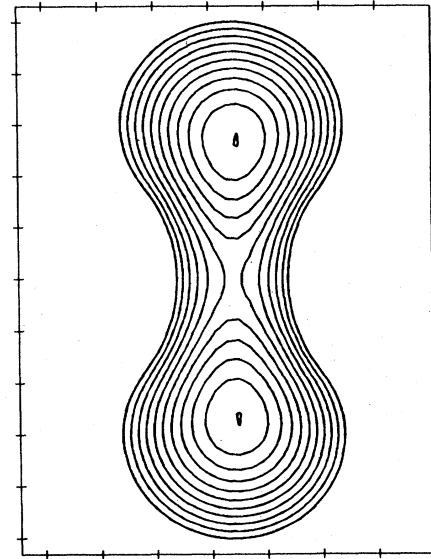


FIG. 10. Relaxed profile in multipinch. $\mu a = 1.5$.

example of the relaxed state at $\mu a = 1.5$ is shown in Fig. 10 (Taylor and Turner, 1985; La Haye *et al.*, 1986). This configuration is symmetric in the upper and lower halves of the cross section, and B_ϕ is of the same sign everywhere.

Similarly the eigenfunctions, Eq. (5.7), can also be compared. The lowest eigenvalue is found to be $\mu a = 2.21$ (La Haye *et al.*, 1986). The corresponding eigenfunction, shown in Fig. 11, is antisymmetric in the two halves of the cross section, i.e., B_ϕ is of opposite sign in the upper and lower halves.

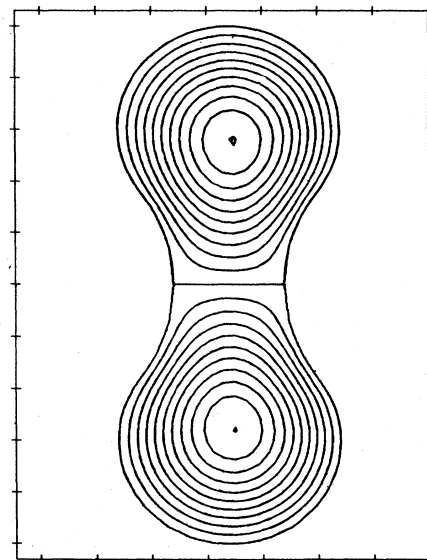


FIG. 11. Eigenfunction for multipinch. $\mu a = 2.21$.

The axisymmetric relaxed states can also be described in terms of the toroidal field. The function f satisfies

$$\Delta^+ f + \mu^2 f = 0 \quad (5.8)$$

with f constant around the boundary. In this description there is no direct reference to the toroidal flux Ψ , which must be introduced through the requirement that

$$\langle f \rangle = \frac{\langle R \rangle \Psi}{A} \quad (5.9)$$

In terms of f the associated eigenvalue problem is also described by (5.8) with f constant on the boundary—so there may appear to be no eigenvalue condition. In fact this arises from the vanishing-flux condition

$$\langle f \rangle = 0. \quad (5.10)$$

One now sees that it is important to distinguish between this eigenvalue problem (problem A) and the simpler eigenvalue problem defined by Eq. (5.8) with $f = \text{zero}$ on the boundary (problem B). Problem A is entirely equivalent to Eq. (5.7), and its lowest eigenvalue determines the point of current saturation. An eigenvalue of problem B, on the other hand, only determines a point at which the toroidal field vanishes at the wall, i.e., a point of “field reversal” $F=0$.

The two eigenvalue problems A and B are quite distinct. However, when there is an equatorial plane of symmetry some of the eigenfunctions χ_i for problem A are antisymmetric about this plane. For such eigenfunctions $\langle \chi_i \rangle = 0$, so Eq. (5.7) and its boundary condition (problem A) are then identical with Eq. (5.8) and its boundary condition (problem B). Consequently the two problems then have a common solution and a common eigenvalue.

This coincidence occurs in the multipinch, where the lowest eigenvalue ($\mu a = 2.21$) of problem A (determining current saturation) coincides with the second-lowest eigenvalue of problem B. Furthermore, this second eigenvalue of problem B is very close to the first, which determines field reversal. [The first and second eigenvalues of problem B differ by less than 2% (Taylor and Turner, 1985): they would be exactly degenerate if the gap between the two lobes of the figure eight were infinitesimal.] As a result, field reversal and current saturation are almost coincident in the multipinch.

We can now describe the properties expected for relaxed states in the multipinch. For small values of K/ψ^2 (low volt-seconds), the relaxed state is axisymmetric and symmetric about the equatorial plane. In this state μa and the plasma current increase with volt-seconds. However, when μa reaches 2.21 the relaxed state changes to one that is no longer symmetric about the equatorial plane (i.e., more current flows in one lobe of the figure eight than the other), although it remains axisymmetric. This “up-down” asymmetry increases with increasing volt-seconds, but μa and the total current are fixed and $F = B_\phi(\text{wall})/\langle B_\phi \rangle$ is almost zero.

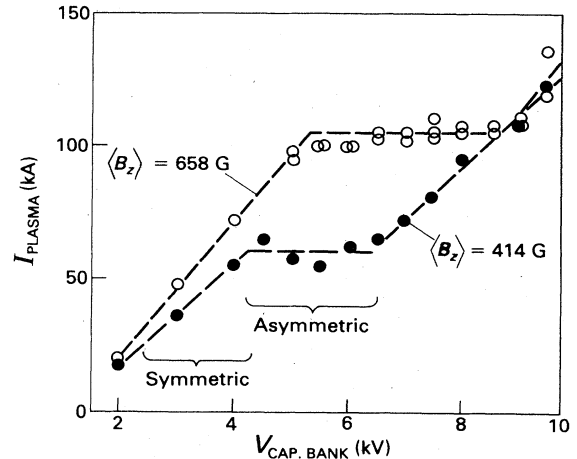


FIG. 12. Plasma current vs driving voltage in multipinch (from La Haye *et al.*, 1986).

These features of the relaxed state are all clearly demonstrated in the multipinch experiment. Figure 12 (La Haye *et al.*, 1986) shows the peak plasma current I_p (at fixed toroidal flux $\langle B_z \rangle$) as a function of the capacitor-bank voltage V_{CB} (the voltage applied to the primary circuit of which the plasma forms the secondary; K/ψ^2 increases roughly linearly with V_{CB}). At low voltage the configuration is axisymmetric and symmetric about the equatorial plane, and the current increases with V_{CB} . At higher V_{CB} the current saturates, and the discharge acquires an “up-down” asymmetry which increases with further increase in V_{CB} . The current saturation and the onset of “up-down” asymmetry almost coincide with vanishing toroidal field at the wall, i.e., with $F=0$.

It can also be seen from Fig. 12 that the saturation current depends on $\langle B_z \rangle$, i.e., on the toroidal flux Ψ . The variation of saturation current with toroidal flux is shown in Fig. 13. The straight line corresponds to $\mu a = 2.42$ and is thus in very good agreement with the calculated theoretical value $\mu a = 2.21$.

One may now ask why current saturation is more clearly demonstrated in the multipinch than in the circular-cross-section pinch. This is probably because in the circular pinch the current-saturated state is reached well after toroidal field reversal, and so involves reverse toroidal current flow near the wall and strong plasma-wall interaction. [See also Mannheimer (1981).] Such currents are inhibited by the low plasma conductivity in this region. On the other hand, because of the near coincidence between toroidal field reversal and current saturation, no such reverse current is called for in the multipinch.

In theory, the up-down asymmetry of the multipinch in the current-saturated state should increase indefinitely with increasing voltage, until eventually the current in one half of the cross section would be reversed. In practice the asymmetry increases until the current in one half falls to zero and the discharge is entirely confined to the other half. From that point on it acts as a circular-cross-section

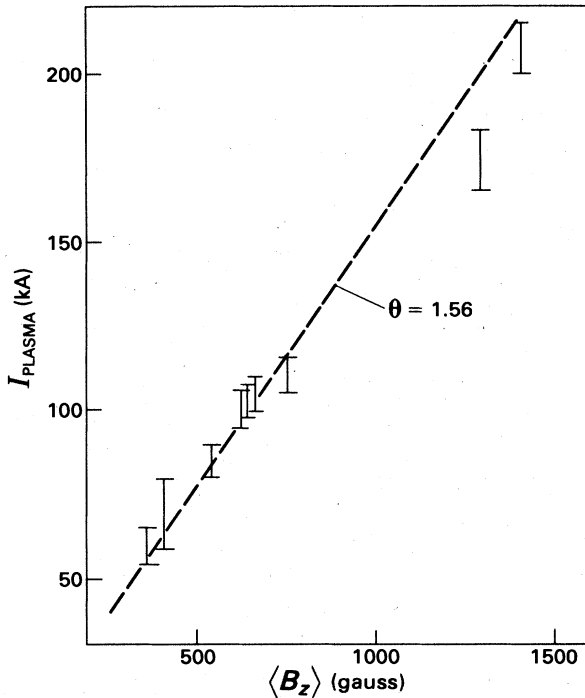


FIG. 13. Variation of I_{sat} with toroidal flux in multipinch. $\theta = 1.56$ corresponds to $\mu a = 2.42$ in this configuration (from La Haye *et al.*, 1986).

discharge confined to one half of the machine—with the other half acting somewhat as an external inductance.

VI. RELAXED STATES IN OTHER SYSTEMS

A. Spheromak

So far we have considered relaxation only for toroidal systems. However, relaxed states are of equal importance in another class of plasma configurations, of which the prototype is the spheromak, Fig. 14. In this configuration (Rosenbluth and Bussac, 1979), the magnetic field has nested toroidal surfaces surrounding a magnetic axis as in a toroidal pinch, but the confining shell is topologically spherical instead of toroidal. (Of course, although the spherical topology is essential, the actual shape need not be a true sphere.)

The essential distinguishing feature of a spheromak is that there is no central aperture for toroidal field coils: consequently the toroidal field is zero everywhere on the wall, and in this respect the spheromak resembles a toroidal pinch at the point of field reversal, with $F=0$. However, in the pinch the vanishing toroidal field implies that $q(\psi)$ is zero at the wall, whereas in the spheromak this is not the case. In fact, for a truly spherical system, $q(\psi)$ decreases only from 0.825 on the magnetic axis to 0.72 at the wall (Rosenbluth and Bussac, 1979). [The quantity $q(\psi)$ is the winding number of the lines of force on the toroidal flux surface ψ ; i.e., $2\pi q$ is the toroidal an-

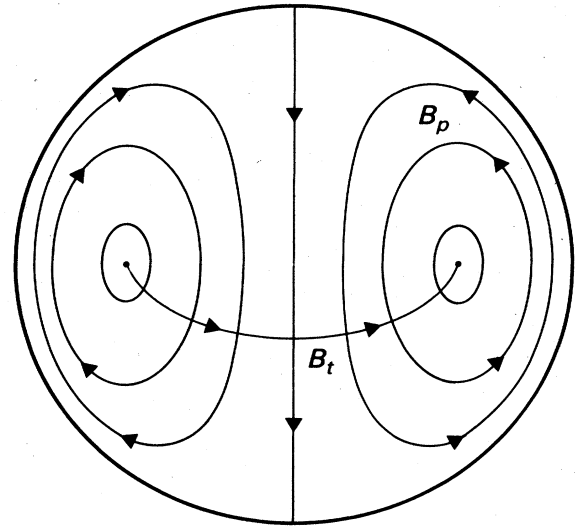


FIG. 14. Spheromak configuration. Schematic.

gle turned through, following a field line, for each complete rotation about the magnetic axis. Because $q(\psi)$ involves an average over the flux surface, it remains finite even though the toroidal field tends to zero over part of the surface.]

Plasma formation in the spheromak is considerably more difficult to visualize than it is in the toroidal pinch (Furth, 1981; Goldenbaum, 1982). In one method, used in the CTX, Beta II, and CTCC-1 experiments (Jarboe *et al.*, 1980, 1983; Turner *et al.*, 1981, 1983; Nagata *et al.*, 1985), a plasma is produced by a coaxial plasma gun and injected into a confinement chamber (Fig. 15). Plasma formed in the gun carries both poloidal field, provided by coils in the gun, and toroidal field produced by plasma currents. The magnetic forces eject the plasma from the gun into the container (known as the flux conserver), where it relaxes into a spheromak configuration. Another method for forming a spheromak plasma employs a combination of θ - and z -pinch discharges, as in the PS-1 experiment (Goldenbaum *et al.*, 1980; Nogi *et al.*, 1980; Bruhns *et al.*, 1983). This process is illustrated in Fig. 16.

Spheromak plasmas can also be formed by a slow inductive process, as in the S-1 experiment (Fig. 17; Yamada *et al.*, 1981). An initial poloidal field is generated by current in a ring-shaped (toroidal) flux core and is weakened on the small-major-radius side of the core by an externally generated vertical field. The flux core also contains a toroidal solenoid, which generates a toroidal flux within it. When this toroidal solenoid is energized it induces poloidal current in plasma surrounding the ring. The associated toroidal field distends the plasma, stretching it towards the axis. Then the toroidal current in the flux core is reversed and additional toroidal current is induced in the plasma. Reconnection of the poloidal field occurs, and a separated plasma toroid is created on the

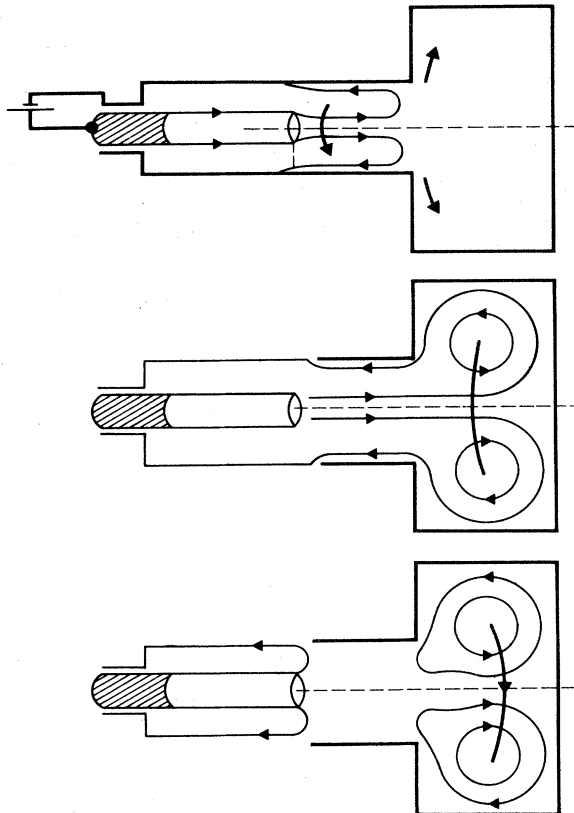


FIG. 15. Spheromak formation by plasma gun (from Turner *et al.*, 1983).

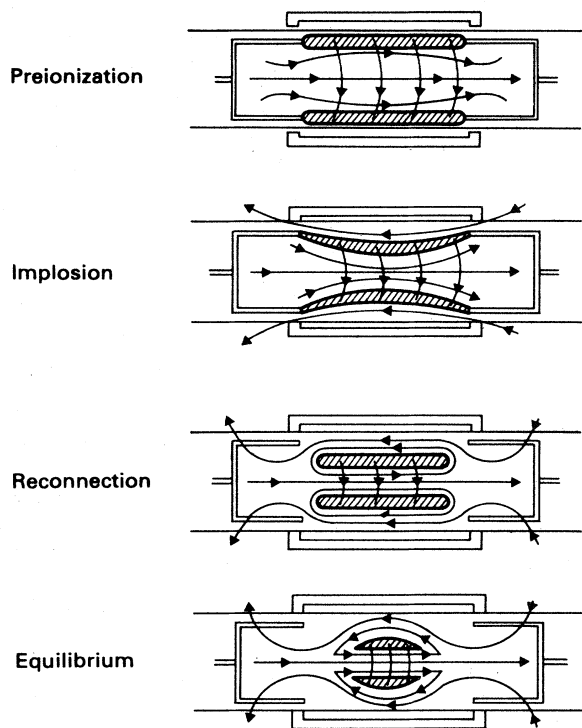


FIG. 16. Spheromak formation by combined θ - z discharge (from Goldenbaum *et al.*, 1980).

small-major-radius side of the flux core. This toroid, the desired spheromak configuration, is held in equilibrium by the external vertical field.

The parameters of several spheromak experiments are shown in Table II. The references cited should be consulted for more details.

1. Relaxed states of spheromak

As in the toroidal systems, the helicity $K_0 = \int \mathbf{A} \cdot \mathbf{B} d\tau$ is conserved during relaxation in the spheromak, and the relaxed state satisfies

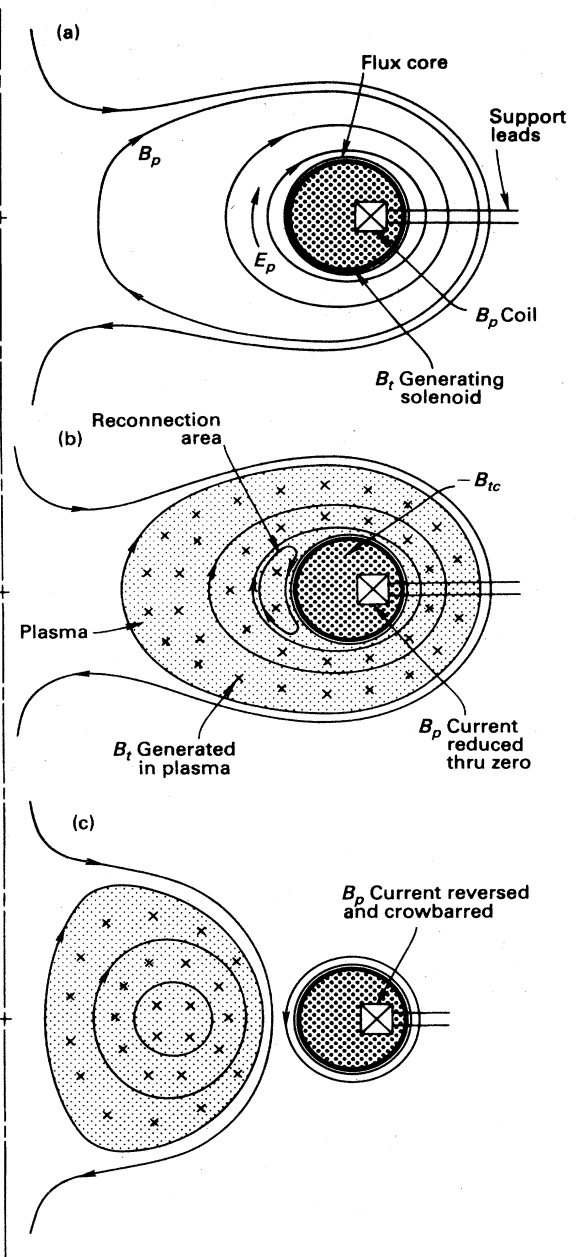


FIG. 17. Spheromak formation by inductive flux core (S-1) (from Yamada *et al.*, 1981).

TABLE II. Spheromak experiments. Representative parameters.

	PS-1 ^a	CTX ^b	S-1 ^c	BETA II ^d	CTCC-1 ^e	HSE ^f	CØP ^g
Flux container (cm)	6×14	30×40	30×55	40×40	20×25	6×9	4×8
I_{max} (kA)	130	500	300	330	100	240	20
T_e (eV)		150	110	10	40	10	10

^aGoldenbaum *et al.* (1980).
^bJarboe *et al.* (1980,1984).
^cYamada *et al.* (1981,1985).
^dTurner *et al.* (1983).
^eNagata *et al.* (1985).
^fBruhns *et al.* (1984).
^gKawai and Pietrzyk (1981).

$$\nabla \times \nabla \times \mathbf{A} = \mu \nabla \times \mathbf{A} \tag{6.1}$$

Despite this formal similarity, however, there is a significant difference between the theory of relaxed states in the spheromak and in the toroidal pinch. In a toroidal device there are two invariant quantities, the helicity K and the toroidal flux ψ , and, as we have seen, these are just sufficient to determine the relaxed state. In the spheromak, toroidal flux ψ is not a conserved quantity; annihilation and creation of flux can occur at the axis of symmetry. Consequently one has only a single invariant K from which to determine the relaxed state.

On the other hand, the spheromak is a singly-connected volume, and $\oint \mathbf{A} \cdot d\mathbf{s}$ vanishes over any closed path in the bounding surface. Apart from a gauge transformation this is equivalent to setting $\mathbf{A}=0$ on the boundary, so that the only possible solutions of Eq. (6.1) for a spheromak are eigenfunctions, and the only possible values for μ are the corresponding eigenvalues.

It is therefore much simpler to find the relaxed state in a spheromak than in a toroidal pinch. There is no need to select from different types of solution; the relaxed state is just the eigenfunction corresponding to the smallest eigenvalue of Eq. (6.1). The value of μ and the field profiles are thus determined by the shape of the container alone. The role of the single invariant K is only to fix the magnitude of the magnetic field, and the toroidal flux ψ plays no direct role in determining the relaxed state.

The axisymmetric eigenfunctions for spheromak systems are easily found. The magnetic field is again expressed in the form (5.1), and the eigenvalue problem for a spheromak reduces to

$$\Delta^+ \chi_i + \mu_i^2 \chi_i = 0 \tag{6.2}$$

with $\chi_i=0$ on the boundary. For simple containers the eigenfunctions can be obtained analytically, and for more complex shapes they are readily computed.

In a spherical container of radius a , the lowest eigenvalue is given by $\mu a = 4.49$, and the corresponding eigenfunction is

$$B_r = 2B_0 [j_1(\mu\rho)/\mu\rho] \cos\theta ,$$

$$B_\varphi = B_0 j_1(\mu\rho) \sin\theta , \tag{6.3}$$

$$B_\theta = -B_0 \frac{d}{d\rho} [\rho j_1(\mu\rho)] \sin\theta ,$$

where ρ, θ, φ are spherical coordinates and $j_1(x) = J_{3/2}(x)/x^{1/2}$ (Rosenbluth and Bussac, 1979).

In a cylindrical container of height h and radius a the lowest eigenvalue is

$$\mu = \left[\left(\frac{3.83}{a} \right)^2 + \left(\frac{\pi}{h} \right)^2 \right]^{1/2} \tag{6.4}$$

(for h/a less than a critical value, see below), and the corresponding eigenfunction is

$$\begin{aligned} B_r &= -B_0 k J_1(lr) \cos(kz) , \\ B_\varphi &= B_0 \mu J_1(lr) \sin(kz) , \\ B_z &= B_0 k J_0(lr) \sin(kz) , \end{aligned} \tag{6.5}$$

where $kh = \pi$, $la = 3.83$, and r, φ, z are cylindrical coordinates (Bondeson *et al.*, 1981; Finn *et al.*, 1981).

The eigenfunctions (6.3) and (6.5) are axisymmetric, but it is possible that the lowest eigenvalue may be that of a nonaxisymmetric mode. Whether this is so depends on the shape of the container. For example, in a cylindrical container the axisymmetric eigenfunction described above has the lowest eigenvalue only when $h/a \leq 1.67$. When $h/a > 1.67$ a nonaxisymmetric mode has a lower eigenvalue, and in this case the relaxed state is nonaxisymmetric (Bondeson *et al.*, 1981; Finn *et al.*, 1981).

2. Spheromak experiments

Measurements have been made of relaxed-state plasmas in several spheromak experiments. Some of the data from the Beta-II experiment (which has a roughly cylindrical flux conserver with $h/a \simeq 1$) are illustrated in Fig. 18 (Turner *et al.*, 1983). This shows the measured poloidal and toroidal fields, together with the theoretical profiles for the relaxed state given by Eq. (6.5). The agreement is very satisfactory, particularly in view of the complex way in which the plasma is formed. It should also be noted

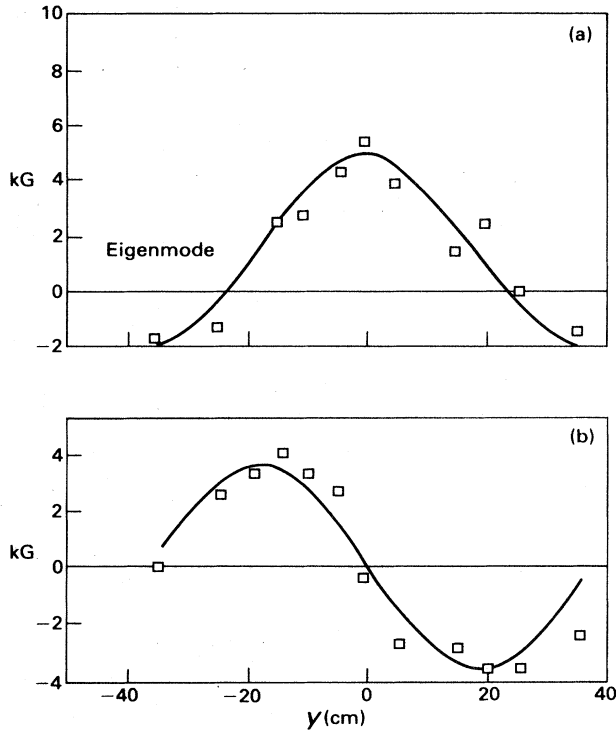


FIG. 18. Magnetic field in BETA II spheromak. Experiment and theory: (a) poloidal field; (b) toroidal field (from Turner *et al.*, 1983).

that the field profiles retained their form, while the energy in the discharge decayed to about one-eighth of its initial value. Furthermore, except for a cutoff when the volt-seconds are too low or the magnetic flux in the gun too high, the initial magnetic flux in the initial relaxed state was proportional to the square root of the helicity produced by the gun—as required by the theory.

Confirmation that $\mu(\equiv \mathbf{j} \cdot \mathbf{B}/B^2)$ is uniform in the relaxed state of a spheromak is provided by Fig. 19 (Hart *et al.*, 1985). This shows the poloidal current versus poloidal flux in the S-1 experiment (which has an ellipsoidal plasma). Not only do the observations lie on a straight line, corresponding to uniform μ , but the slope of the line also agrees well with the calculated value of μa . A more detailed picture of μ is given in Fig. 20, which shows the profile before and after relaxation, as well as the theoretical value.

The most striking feature of S-1, however, occurs during relaxation itself (Janos *et al.*, 1985a, 1985b). Figure 21 shows the evolution of the poloidal and toroidal fluxes, and of q on the magnetic axis during the relaxation phase. This indicates that during relaxation q rises rapidly from its initial very small value to its theoretical predicted value (0.65 for the ellipsoidal configuration of the S-1 plasma). This development is accompanied by destruction of poloidal flux and the spontaneous creation of toroidal flux in a very short time compared with the resistive decay time. Furthermore, following relaxation, q

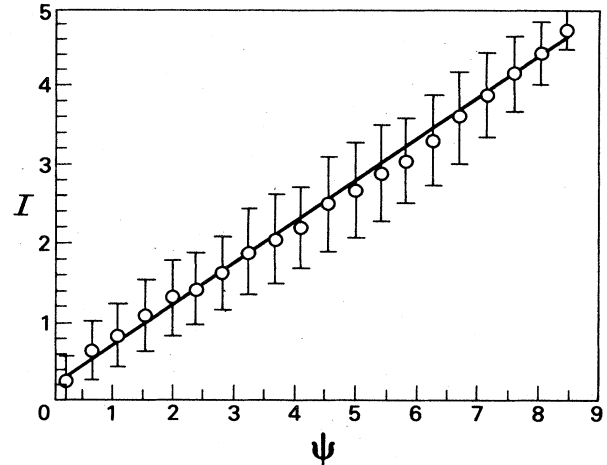


FIG. 19. Poloidal current vs poloidal flux in S-1 spheromak (from Hart *et al.*, 1985).

remains constant during the resistive decay of the plasma, demonstrating the persistence of the relaxed configuration.

B. Flux-core spheromak (FCS)

An interesting development of the spheromak is a configuration obtained from it by introducing a central core of externally produced magnetic flux along the axis of symmetry (Fig. 22). This externally linked flux enters through one polar cap and leaves through the other. [Of course the actual boundary may again depart significantly from the spherical form. See Jensen and Chu (1981, 1983).] Although the FCS may appear to resemble a toroidal pinch, it is in fact completely different. Unlike the toroidal pinch, it has only plasma in the central core, not a fixed conductor; consequently, as in the simple spheromak, the toroidal flux is not a conserved quantity.

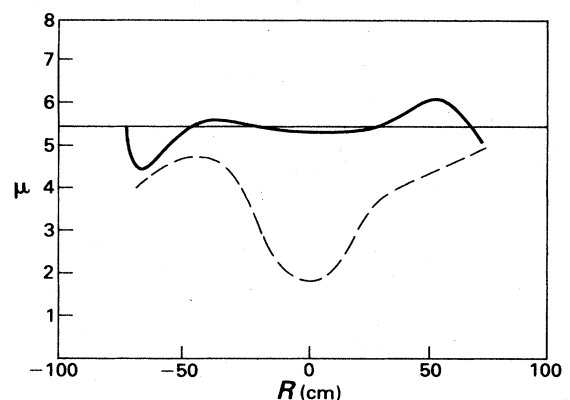


FIG. 20. Measured profile of $\mu(r)$ in S-1 spheromak (from Hart *et al.*, 1985).

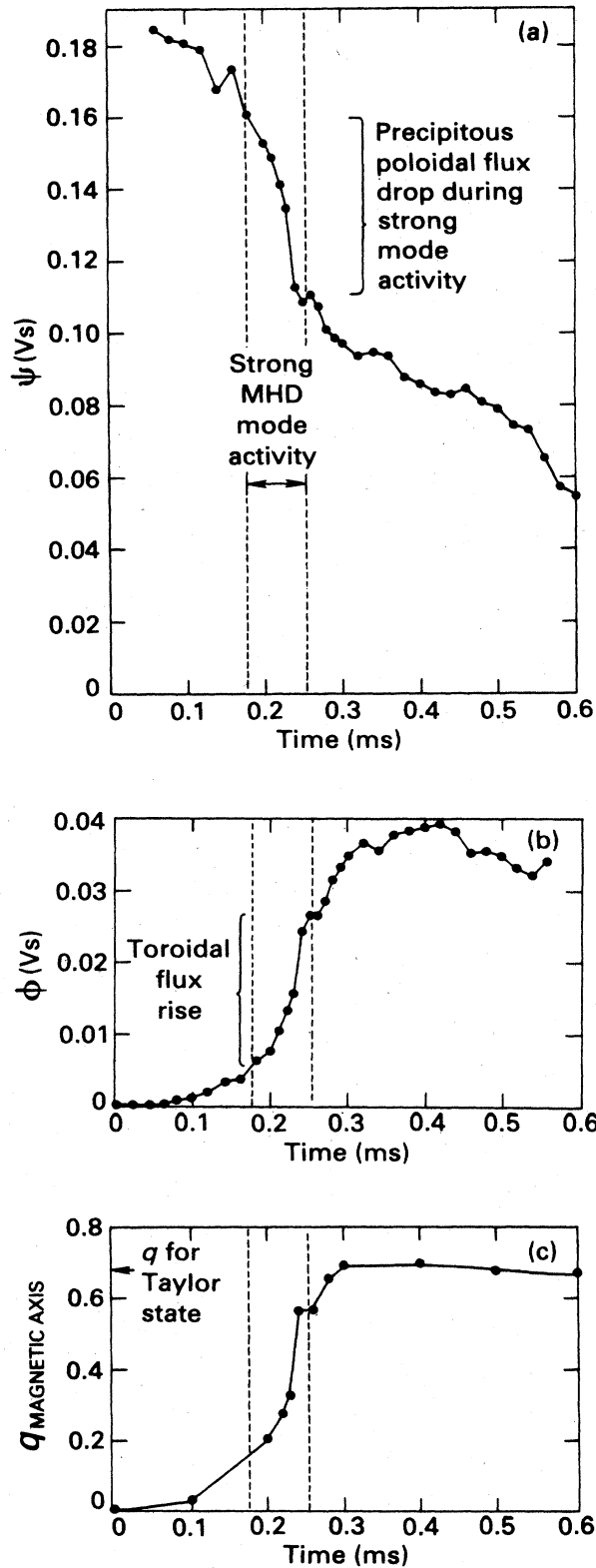


FIG. 21. Time dependence of magnetic fields in S-1 spheromak (from Janos *et al.*, 1985a, 1985b).

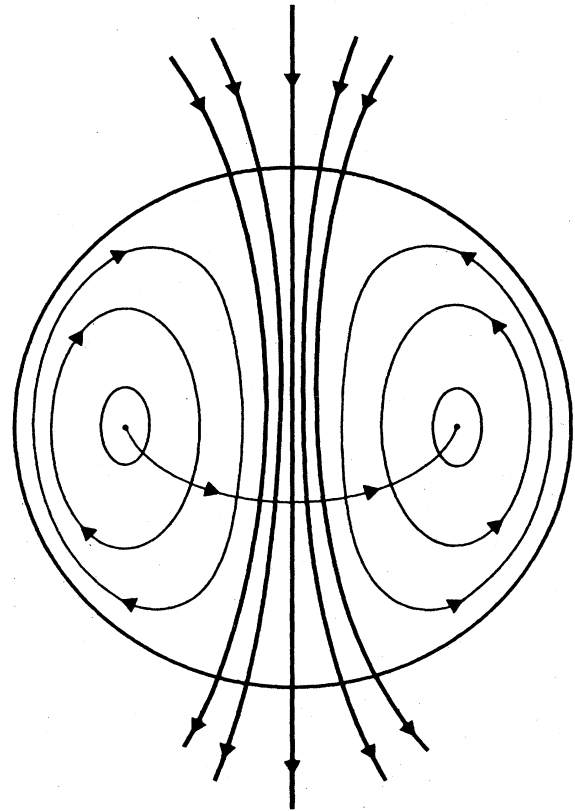


FIG. 22. Flux-core spheromak. Schematic.

1. Relative helicity

In the FCS configuration the plasma container is *not* a flux surface, and we have already noted that in this event the helicity K is not well defined. A modification of the definition of helicity is therefore needed to deal with the flux-core spheromak and similar systems.

One method (Berger and Field, 1984) is to imagine that the flux leaving and entering the boundary is extended outside as a vacuum field ($\nabla \times \mathbf{B} = 0$). Then the total helicity $\int \mathbf{A} \cdot \mathbf{B}$ inside and outside the sphere is a well-defined quantity. Furthermore, if the bounding surface of the sphere is perfectly conducting, the normal component of \mathbf{B} is "frozen in" so that changes in the interior field do not affect the hypothetical field outside. We may then consider the difference in helicity of two fields, which differ inside the spheromak but have identical normal field components on the boundary and hence identical hypothetical extension fields outside. This difference, the relative helicity of the two configurations, is well defined and gauge invariant. (Note that it is necessary to include the contributions to $\int \mathbf{A} \cdot \mathbf{B}$ from both the interior and exterior regions, even though the exterior field does not change. This reflects the fact that helicity is not a local quantity and can be transferred, within a flux surface, from the interior to the exterior of the container by a gauge transformation.)

Of course, to make use of the relative helicity K_R we must show that it is invariant during relaxation. A straightforward calculation gives

$$\frac{dK_R}{dt} = 2 \int_{\text{interior}} \mathbf{E} \cdot \mathbf{B} d\tau + 2 \int_{\text{exterior}} \mathbf{E} \cdot \mathbf{B} d\tau. \quad (6.6)$$

The hypothetical exterior magnetic field is constant during relaxation, so $\nabla \times \mathbf{E} = 0$. Thus $\mathbf{E} = \nabla\varphi$, where φ is a single-valued function and

$$\frac{dK_R}{dt} = 2 \int_{\text{interior}} \mathbf{E} \cdot \mathbf{B} + 2 \oint \varphi \mathbf{B} \cdot d\mathbf{S}. \quad (6.7)$$

When the bounding surface is equipotential, φ is constant over it, and the surface integral vanishes. The interior integral is the usual one for any system and is negligible on the relaxation time scale for a highly conducting plasma ($E_{\parallel} \sim 0$). Consequently K_R is indeed invariant during relaxation.

Equation (6.7) also shows that helicity may be injected or extracted from the FCS if one of the polar caps is electrically insulated and maintained at a different potential from the other. Then helicity is changed at a rate (Taylor, 1975, 1976; Jensen and Chu, 1984)

$$\frac{dK_R}{dt} = 2V_p\psi_p, \quad (6.8)$$

where V_p is the voltage between the polar caps and ψ_p is the flux through them. This provides another method of sustaining a relaxed state against resistive decay. [It also describes the production of helicity in plasma guns (Turner *et al.*, 1983), referred to in Sec. VI.A.2 above.]

2. Relaxed states

The relaxed state of a flux-core system is obtained by minimizing the energy subject to K_R being invariant and with the boundary condition that the normal component of \mathbf{B} be constant. Once again this leads to the equation for relaxed states,

$$\nabla \times \mathbf{B} = \mu \mathbf{B}, \quad (6.9)$$

but for the new system a new interpretation is needed. Before discussing this we should remark that by neglecting all other helicity constraints of the type $K(\alpha, \beta) = \text{const}$ we are implying that in the flux-core spheromak turbulence can produce linking between flux lines that thread the polar caps and those that do not, i.e., the separatrix between the externally linked flux and the internal flux is not preserved during turbulence.

For a flux-core system, one interpretation of Eq. (6.9) closely resembles that for toroidal systems (Sec. III). This is applicable when the plasma relaxes from an initial state with given helicity K_R and given flux ψ_p through the polar caps. Then the value of μ is determined by the ratio K_R/ψ_p^2 (in rather the same way as the symmetric state of a toroidal pinch is determined by K/ψ^2), and the magnitude of the field is determined by ψ_p , so that the relaxed

state is fully determined by the two invariants K and ψ_p . This interpretation assumes that the polar caps can supply whatever current is required in the relaxed state; if they cannot do so, the resulting voltage drop would reduce the helicity until the relaxed state corresponded to the current available.

The fact that voltages on the polar caps can change the helicity leads to a second interpretation of Eq. (6.9) for the FCS systems. If one of the polar caps, say that in which $B_n > 0$, is electrically insulated from the rest of the container (e.g., by a thin annular gap) and connected to a suitable circuit, then μ can be controlled by the current I_p through it; $\mu = I_p/\psi_p$. (The magnitude of the field is still determined by the polar-cap flux ψ_p .) This view of Eq. (6.9) describes a steady-state FCS in which initial conditions are no longer significant. The helicity K_R is not then independently specified, but reaches the value required to conform with μ —through a balance between helicity injection (or extraction) and resistive dissipation.

A computed field profile for a spherical FCS system is shown in Fig. 23 (Taylor and Turner, 1985). Analytic solutions for an idealization in which the polar caps are shrunk to polar points (though retaining finite flux through them) are shown in Fig. 24 (Turner, 1984). This illustrates some interesting changes that occur in the FCS configuration as the ratio I_p/ψ_p , and hence μ , is increased. When I_p/ψ_p is much smaller than the lowest eigenvalue for the configuration ($\mu_s = 4.49/a$), the externally linked flux (and current) forms a large part of the total flux (and current) in the system. As I_p/ψ_p ap-

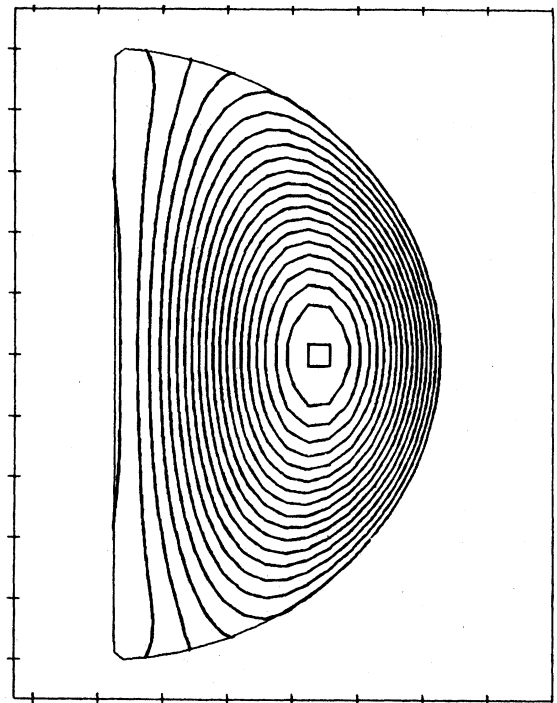


FIG. 23. Computed field in flux-core spheromak. $\mu a = 4.09$.

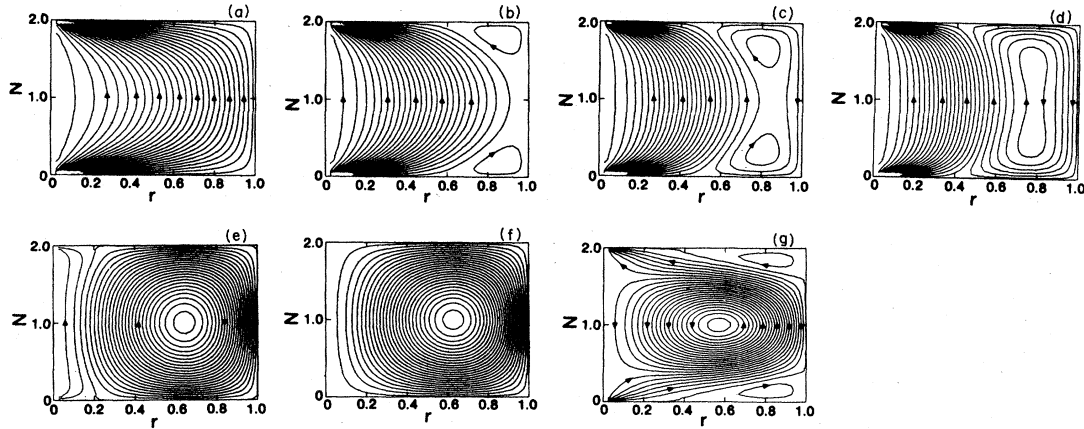


FIG. 24. Field in idealized flux-core spheromak at various values of μa : (a) $\mu a = 0.001$; (b) $\mu a = 2.25$; (c) $\mu a = 2.70$; (d) $\mu a = 3.00$; (e) $\mu a = 4.00$; (f) $\mu a = 4.14$; (g) $\mu a = 5.00$ (from Turner, 1984).

proaches the eigenvalue μ_s , the ratio of self-generated flux (and current) to the externally linked flux (and current) increases indefinitely, and the externally linked flux is confined to a slim pencil along the axis of the plasma—which otherwise is identical to that in a simple spheromak. As I_p/ψ_p increases beyond μ_s , the configuration switches to one in which the externally linked flux passes around the *outside* of the spheromak. [However, one would not expect this to be a true lowest-energy state (see Secs. VII and IX).]

The ratio of the self-generated poloidal flux to the externally linked flux defines a flux magnification ratio $M(\mu)$ which could be used to characterize FCS experiments in somewhat the same way as $F(\theta)$ (the toroidal field ratio) is used to characterize RFP experiments.

3. Experiments

Flux-cored configurations have been produced in the PS-1 experiment (Bruhns *et al.*, 1983) and in the CTX experiment (Jarboe *et al.*, 1983; Jarboe, 1985a). The latter experiment is particularly interesting, as it has also demonstrated the sustainment of the spheromak plasma by a voltage across the polar caps—though in a much distorted form. A schematic diagram of the configuration of the sustained plasma in the CTX experiment is shown in Fig. 25. It can be seen that there is a core of flux (shown by hatched lines), which passes from the inner electrode of the gun, along the axis of the spheromak plasma, and returns around it to the outer gun electrode. From the point of view of the plasma the gun voltage therefore appears across the flux core—though the “polar caps” are somewhat distant. The configuration shown has been sustained by the gun voltage for much longer than the normal resistive decay time of the magnetic fields.

Recognition that near-relaxed-state plasmas can be maintained in this way has opened up new possibilities and led to the investigation of configurations in which the

source of helicity is still more distant from the plasma containment region (Barnes *et al.*, 1985; Jarboe, 1985b; Platts *et al.*, 1985; Wright *et al.*, 1985). An example is shown schematically in Fig. 26. A remarkable feature of these experiments is that not only was a spheromak plasma successfully created in the flux conserver, but the plasma in the connecting tube between flux conserver and source also showed the characteristics of the helical $m = 1, ka = 1.25$ relaxed state in a cylinder.

VII. STABILITY OF RELAXED STATES

It is clear that, because they are states of minimum energy, all relaxed states are stable against perturbations that leave helicity invariant. This includes all ideal magnetohydrodynamic perturbations.

The stability of the relaxed states was verified directly (Taylor, 1974b; see also Schmidt, 1966; Kruger, 1976a, 1976b) by considering the second variation of mag-

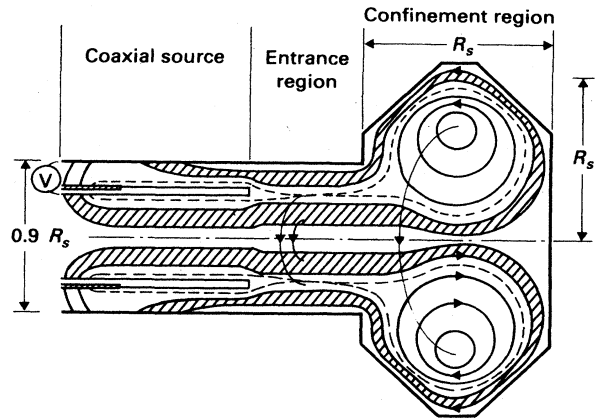


FIG. 25. Sustained configuration in CTX experiment (from Jarboe, 1985a, 1985b).

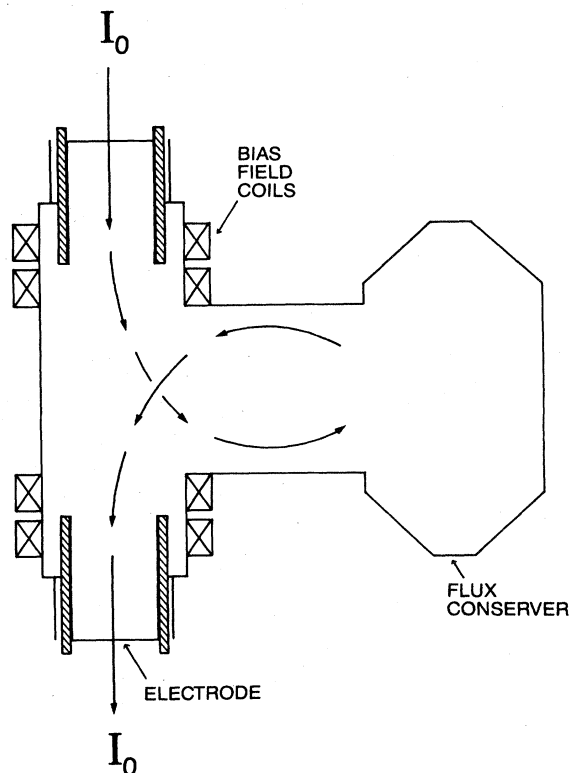


FIG. 26. Experiment with remote helicity injection (from Jarboe, 1985a, 1985b).

netic energy, produced by a perturbation $\delta\mathbf{A}$ about the equilibrium relaxed state,

$$\delta W_2 = \frac{1}{2} \int (\nabla \times \delta\mathbf{A})^2 d\tau - \frac{\mu}{2} \int \delta\mathbf{A} \cdot \nabla \times \delta\mathbf{A} d\tau. \quad (7.1)$$

If we use the normalization

$$\frac{1}{2} \int (\nabla \times \delta\mathbf{A})^2 d\tau = 1 \quad (7.2)$$

and the boundary condition $\delta\mathbf{A} = 0$, then the minimizing perturbation satisfies

$$\nabla \times \nabla \times \delta\mathbf{A} - \frac{\mu}{(1-g)} \nabla \times \delta\mathbf{A} = 0. \quad (7.3)$$

The corresponding perturbation in energy is

$$(\delta W_2)_{\min} = \frac{g}{2} \int (\nabla \times \delta\mathbf{A})^2 d\tau. \quad (7.4)$$

Comparing Eq. (7.3) with the eigenvalue equation (4.2), we see that $g \geq 0$ if $\mu \leq$ the lowest eigenvalue for the problem—as is the case for all minimum-energy relaxed states—so that $\delta W_2 \geq 0$.

Since this discussion does not require the fluid displacement ξ to be finite, it applies to resistive tearing modes as well as ideal modes (Taylor, 1976; Rosenbluth and Busac, 1979). Consequently relaxed states are also stable to resistive tearing modes. This is illustrated by the result obtained (in Sec. III) for the large-aspect-ratio circular-

cross-section toroidal pinch. The point at which the lowest-energy state ceases to be the axisymmetric configuration occurs at $\mu a = 3.11$. This is precisely the point at which the axisymmetric configuration becomes linearly unstable to a resistive tearing mode (Whiteman, 1962; Gibson and Whiteman, 1968). [Ideal magnetohydrodynamic instability does not arise until $\mu a = 3.18$ (Voslamber and Callebaut, 1962).]

As one would expect, therefore, the change from the symmetric relaxed state to the helical relaxed state corresponds to a bifurcation, in which linear stability is transferred from one relaxed state to the other. However, it is important to realize that the theory of relaxed states goes beyond the linear theory. The helical deformation that occurs is *fully* determined (by K/ψ^2), and in this respect the present theory provides a *nonlinear* description of the resistive tearing mode (Martin and Taylor, 1974).

VIII. SUMMARY AND CONCLUSIONS

In this paper we have described the concept of plasma relaxation by reconnection of magnetic lines of force. This is brought about by plasma turbulence in the presence of small resistivity and leads to a unique lowest-energy relaxed state. In this process magnetic helicity plays a vital role as a unique invariant. We should emphasize that, because it is driven by turbulence, this relaxation occurs on a much shorter time scale than normal resistive diffusion, and it is only on this shorter time scale that the magnetic helicity K is invariant. On the longer resistive time scale, energy and helicity will both decay unless deliberately sustained. Resistive decay usually causes the configuration to evolve away from the fully relaxed state, and in that event periodic or continuous secondary relaxations occur to maintain the profile close to a relaxed configuration. Similar minor relaxations must occur when the discharge is sustained by helicity injection. Another feature that should be emphasized is that relaxation is *not* a passive decay process. It involves the self-generation of fields and currents by plasma turbulence.

We have also described the calculation of the relaxed state in various systems. In all cases it satisfies Eq. (1.8), but the interpretation of this equation and the manner in which the appropriate solution is selected depend on the topology of the system and on the boundary conditions. Consequently there are several different types of relaxed state, each with its own distinct characteristics.

In parallel with the theoretical discussion, we have reviewed some of the experimental evidence for relaxed states. Configurations close to those predicted are almost universally observed in toroidal pinches, in the multipinch, in spheromaks, and in flux-core systems. [In tokamaks the disruption phenomena are also an example of relaxation, in which the theory correctly predicts the negative voltage spike. A well-known model of sawtooth oscillations in tokamaks (Kadomtsev, 1975, 1977) is also closely related to relaxation. However, apart from disrup-

tion and sawtooth oscillation, relaxation does not appear to play a dominant role in tokamaks. This is presumably due to the strong toroidal magnetic field and the care taken to avoid instability and turbulence.]

The experiments provide quantitative verification of the distinct characteristics of the different types of relaxed state. These include such features as field reversal and current saturation in the toroidal pinch, and in a different form in the multipinch, as well as flux annihilation and generation in the spheromak and flux-core systems.

The remarkable success of the theory gives added impetus to investigations of the precise mechanism of relaxation and of the associated flux generation—sometimes called dynamo action. (The mechanism may be different in different circumstances—only the final state is unique.) This problem is, of course, part of the notoriously difficult problem of plasma turbulence. In addition to the numerical simulations referred to in Sec. I.C, several models of plasma turbulence have been discussed in the literature, and in some cases these lead to the relaxed state, but the subject is far from complete. The reader should consult, for example, Frisch *et al.* (1975), Moffatt (1978), Montgomery *et al.* (1978), Mattheus and Montgomery (1980a,1980b), Riyopoulos *et al.* (1982), Turner (1983), Ting *et al.* (1986).

A related question is that of deviations from the fully relaxed profile. We have mentioned that in the RFP $\mu \equiv \mathbf{j} \cdot \mathbf{B} / B^2$ (which is uniform in a fully relaxed state) falls off in the vicinity of the wall. This is presumably due to the high plasma resistivity near the wall, which the relaxation mechanism, or dynamo process, is unable fully to overcome. In investigating this, experiments of the flux-core-spheromak type seem particularly useful, since one can control the relaxed state and change from one relaxed state to another by injecting helicity. Furthermore, by having two pairs of electrodes instead of a single pair of polar caps one could maintain a partially relaxed state.

ACKNOWLEDGMENTS

I should like to thank my colleagues for many useful discussions on the topics in this paper. In particular, I am indebted to Torkil Jensen and M. S. Chu for valuable discussions on the general relaxed state, to R. La Haye for providing data on the multipinch, to M. Yamada for data on the S-1 spheromak, and to H. Bodin and A. Newton for frequent guidance on toroidal pinch experiments. In addition, M. Bevir, C. Gimblett, T. Jarboe, D. Montgomery, A. Reiman, L. Turner, and others have provided helpful comments and criticisms.

APPENDIX A: GENERAL THEORY OF RELAXED STATES

1. Toroidal systems

The theory of relaxed states in a general toroidal system is similar to that for the large-aspect-ratio system

described in Sec. III. The general theory has been discussed by Jensen and Chu (1984), whose description is followed in this section, but with some additional new features. A more mathematical view of some aspects of this problem can be found in Faber *et al.* (1982,1985).

In a general toroidal system the relaxed state is found by minimizing

$$W = \frac{1}{2} \int (\nabla \times \mathbf{A})^2 d\tau \tag{A1}$$

over all variations $\delta \mathbf{A}$ of the vector potential that leave the helicity

$$K_0 = \int \mathbf{A} \cdot \nabla \times \mathbf{A} d\tau \tag{A2}$$

invariant. Introducing a Lagrange multiplier leads to

$$\delta I = \int \delta \mathbf{A} \cdot (\nabla \times \nabla \times \mathbf{A} - \mu \nabla \times \mathbf{A}) d\tau + \oint \delta \mathbf{A} \times \left[\nabla \times \mathbf{A} - \frac{\mu \mathbf{A}}{2} \right] \cdot d\mathbf{S} . \tag{A3}$$

We assume that at the plasma-wall boundary the normal magnetic field ($\mathbf{n} \cdot \nabla \times \mathbf{A}$) vanishes. This ensures that the helicity is gauge invariant (Sec. I.C) and that δI is also gauge invariant (i.e., $\delta I \equiv 0$ if $\delta \mathbf{A} = \nabla \varphi$). If the wall is perfectly conducting, the condition $\mathbf{E}_{||}(\text{wall}) = 0$ implies that at the boundary $\delta \mathbf{A}_{||}$ is the gradient of a scalar. Writing $\delta \mathbf{A} = \delta \mathbf{A}^* + \nabla \varphi$ where $\delta \mathbf{A}_{||}^*$ vanishes at the boundary, we find that the minimization (A3) leads to the Euler equation

$$\nabla \times \nabla \times \mathbf{A} - \mu \nabla \times \mathbf{A} = 0 . \tag{A4}$$

The specification of the relaxed state is completed by the boundary conditions $\mathbf{n} \cdot \nabla \times \mathbf{A} = 0$ and the given values of the loop integrals $\oint \mathbf{A} \cdot d\mathbf{l}$ and $\oint \mathbf{A} \cdot d\mathbf{s}$.

If we assume that the eigenfunctions of the associated eigenvalue problem

$$\nabla \times \nabla \times \mathbf{a}_i = \lambda_i \nabla \times \mathbf{a}_i , \tag{A5}$$

with boundary condition $\mathbf{a}_i = 0$, form a complete set then, following Jensen and Chu (1984), we may write

$$\mathbf{A} = \mathbf{A}_0 + \sum \alpha_i \mathbf{a}_i , \tag{A6}$$

where \mathbf{A}_0 represents a toroidal *vacuum* field satisfying the boundary conditions of the original problem. Note that an eigenfunction carries no toroidal flux, and in an axisymmetric system the vacuum toroidal field will also be axisymmetric.

The eigenfunctions are orthogonal in the sense that

$$(\lambda_i - \lambda_j) \int \mathbf{a}_j \cdot \nabla \times \mathbf{a}_i = 0 \tag{A7}$$

and

$$\lambda_i \int \mathbf{a}_i \cdot \nabla \times \mathbf{a}_i = \int (\nabla \times \mathbf{a}_i)^2 > 0 , \tag{A8}$$

so that the appropriate normalization is

$$\int \mathbf{a}_i \cdot \nabla \times \mathbf{a}_j = \int \mathbf{a}_j \cdot \nabla \times \mathbf{a}_i = \frac{\lambda_i}{|\lambda_i|} \delta_{ij} . \tag{A9}$$

Then, so long as μ is not equal to an eigenvalue, the coefficients α_i are given by

$$\alpha_i = \frac{\mu}{(\lambda_i - \mu)} \frac{|\lambda_i|}{\lambda_i} I_i, \quad (\text{A10})$$

where

$$I_i = \int \mathbf{a}_i \cdot \nabla \times \mathbf{A}_0 \quad (\text{A11})$$

and the important invariant quantity K/ψ^2 can be expressed as

$$\frac{K}{\psi^2} = \frac{1}{\psi^2} \int \mathbf{A}_0 \cdot \nabla \times \mathbf{A}_0 + \sum_i \frac{\lambda_i}{|\lambda_i|} \frac{I_i^2}{\psi^2} \left[\frac{\lambda_i^2}{(\lambda_i - \mu)^2} - 1 \right]. \quad (\text{A12})$$

This expression depends only on the shape of the toroidal container. It constitutes a relation between K/ψ^2 and the parameter μ . Note that K/ψ^2 diverges when $\mu \rightarrow \lambda_i$ unless $T_i = 0$.

At this point, we depart from Jensen and Chu to recognize that many eigenfunctions may not appear in the expansion (A6). For example, in an axisymmetric system all nonaxisymmetric eigenfunctions [$\sim \exp(in\varphi)$ with $n \neq 0$] are absent, since for them $I_i \equiv 0$. Similarly in the multipinch, I_i also vanishes even for axisymmetric eigenfunctions when these are antisymmetric about the midplane of the cross section. The eigenfunctions for which $I_i \equiv 0$ will be termed decoupled.

With this in mind, we see that in axisymmetric systems the solution

$$\mathbf{A} = \mathbf{A}_0 + \sum_i' \frac{\mu}{(\lambda_i - \mu)} \frac{\lambda_i}{|\lambda_i|} I_i \mathbf{a}_i \quad (\text{A13})$$

(where \sum_i' denotes a sum over coupled eigenfunctions only) represents a solution analogous to the $m=0, k=0$, type-(i) solution in the circular-cross-section torus. For this solution μ is determined, through Eq. (A12), by the value of K/ψ^2 ; such a solution can always be found for some value of μ in the range $\lambda_i^- < \mu < \lambda_i^+$, where λ_i^- is the largest negative eigenvalue and λ_i^+ is the smallest positive eigenvalue. For a system that has mirror symmetry about any plane, the eigenvalues occur in pairs, $\pm \lambda_i$; consequently it is often sufficient to discuss only positive eigenvalues.

When μ is equal to one of the decoupled eigenvalues λ_j , an arbitrary multiple of the corresponding decoupled eigenfunction can be added to Eq. (A13), and it will remain a solution of Eq. (A4) satisfying the boundary conditions. Thus another solution is given by

$$\mathbf{A} = \mathbf{A}_0 + \sum_{i \neq j}' \frac{\lambda_i \lambda_j}{|\lambda_i| (\lambda_i - \lambda_j)} I_i \mathbf{a}_i + \beta \mathbf{a}_j, \quad (\text{A14})$$

where the sum is again over coupled eigenfunctions only.

This solution is valid only for $\mu = \lambda_j$, and K/ψ^2 , now given by

$$\frac{K}{\psi^2} = \frac{1}{\psi^2} \int (\mathbf{A}_0 \cdot \nabla \times \mathbf{A}_0) d\tau + \sum_{i \neq j} \frac{\lambda_i}{|\lambda_i|} \frac{I_i^2}{\psi^2} \frac{2\lambda_i - \lambda_j}{(\lambda_i - \lambda_j)^2} + \frac{\beta^2}{\psi^2} \frac{\lambda_j}{|\lambda_j|}, \quad (\text{A15})$$

determines the coefficient β . These solutions are analogous to the type-(ii) mixed solutions of the circular plasma.

Noting that the lowest-energy solution is that with the smallest $|\mu|$ (see below), we can now summarize the general relaxed states of axisymmetric systems as follows. (For simplicity, we consider that μ and K are positive and the expression "lowest eigenfunction" means the one with the smallest positive eigenvalue.)

If the lowest eigenfunction is decoupled, then there are two candidates for the lowest-energy relaxed state. The first exists for a continuous range of μ , from zero to the lowest eigenvalue λ_0 . It is the appropriate solution when K/ψ^2 is small and μ is then determined by, and increases with, K/ψ^2 . The second candidate is a superposition of the first solution and the lowest eigenfunction. It exists only for $\mu = \lambda_0$ and is the appropriate solution when K/ψ^2 is such that μ would exceed λ_0 in the first solution. In this event μ is fixed at λ_0 and is no longer determined by K/ψ^2 ; instead K/ψ^2 determines the amplitude of the eigenfunction component. In this solution the toroidal current, at fixed toroidal flux, is independent of volt-seconds.

As we have noted, in axisymmetric systems the lowest eigenfunction is usually decoupled and the above description applies. If the lowest eigenfunction is *not* decoupled, then only the first solution exists and μ is *always* determined by K/ψ^2 . However, as the lowest eigenvalue is approached $K/\psi^2 \rightarrow \infty$, so that even in this situation μ can never exceed the lowest eigenvalue (Jensen and Chu, 1984). In this regard, therefore, there is little distinction between the behavior of systems whose lowest eigenfunction is decoupled and those in which it is coupled—especially if the coupling is weak.

2. Spherical systems

For a general (topologically) spherical system whose boundary is a flux surface, the relaxed state is again given by Eq. (A4). However, a spherical system is singly connected, and all loop integrals $\oint \mathbf{A} \cdot d\mathbf{s}$ are zero. Apart from a gauge transformation, this is equivalent to $\mathbf{A} = 0$ on the boundary, so that the *only* relaxed states in spherical systems are the eigenfunctions. The lowest-energy relaxed state is just the lowest eigenfunction. Consequently, as noted in Sec. VI, μ and the field profiles are determined by the shape of the container alone. The invariant K determines only the magnitude of the field, and there is no invariant toroidal flux.

APPENDIX B: LOWEST-ENERGY STATE VERSUS μ

In determining the lowest-energy relaxed state there is a useful relation between the difference in energy of two states of given helicity and the difference in μ for the two states (Martin and Taylor, 1974; Taylor, 1975; Reimann, 1980,1981; Faber *et al.*, 1982).

Suppose we have two solutions \mathbf{A}_1 and \mathbf{A}_2 (corresponding to μ_1 and μ_2) of Eq. (A4), which have the same helicity K and satisfy the same boundary conditions. Then, apart from a gauge transformation, $\mathbf{A}_1 = \mathbf{A}_2$ on the boundary, and one can verify the following identities:

$$\int [\nabla \times (\mathbf{A}_2 - \mathbf{A}_1)]^2 = (\mu_2 + \mu_1) \int (\mathbf{A}_2 - \mathbf{A}_1) \cdot \nabla \times \mathbf{A}_2, \quad (\text{B1})$$

$$\int (\nabla \times \mathbf{A}_2)^2 - \int (\nabla \times \mathbf{A}_1)^2 = (\mu_2 - \mu_1) \int (\mathbf{A}_2 - \mathbf{A}_1) \cdot \nabla \times \mathbf{A}_2. \quad (\text{B2})$$

Consequently, if W_1 and W_2 denote the energy of the two solutions,

$$W_2 - W_1 = \frac{\mu_2 - \mu_1}{\mu_2 + \mu_1} \int \frac{(B_2 - B_1)^2}{2} \quad (\text{B3})$$

or

$$W_2 - W_1 = \frac{\mu_2^2 - \mu_1^2}{(\mu_2 + \mu_1)^2} \int \frac{(B_2 - B_1)^2}{2}. \quad (\text{B4})$$

Hence, if there are two possible relaxed states [i.e., two solutions of Eq. (A4) with correct helicity], then the lower-energy one is that with the smaller $|\mu|$.

REFERENCES

- Antoni, V., S. Martini, S. Ortolani, and R. Paccagnella, 1983, in *Mirror Based and Field Reversed Approaches to Magnetic Fusion*, proceedings of the International School of Physics Workshop, edited by R. Post, D. E. Baldwin, and D. D. Ryutov [International School of Plasma Physics, Varenna (Como), Italy], p. 107.
- Aydemir, A. Y., and D. C. Barnes, 1984, *Phys. Rev. Lett.* **52**, 930.
- Aydemir, A. Y., D. C. Barnes, E. J. Caramana, A. A. Mirin, R. A. Nebel, D. D. Schnack, and A. G. Sgro, 1985, *Phys. Fluids* **28**, 898.
- Barnes, C. W., H. W. Hoida, I. Henins, J. C. Fernandez, T. R. Jarboe, S. O. Knox, G. J. Marklin, and R. M. Mayo, 1985, *Bull. Am. Phys. Soc.* **30**, 1453.
- Berger, M. A., and G. B. Field, 1984, *J. Fluid Mech.* **147**, 133.
- Bevir, M., and J. Gray, 1980, in *Proceedings of the Reverse Field Pinch Theory Workshop*, edited by H. R. Lewis and R. A. Gerwin (Los Alamos National Laboratory, Los Alamos, New Mexico), Session III, paper A-3.
- Bhattacharjee, A., and R. L. Dewar, 1982, *Phys. Fluids* **25**, 887.
- Bhattacharjee, A., R. L. Dewar, and D. Monticello, 1980, *Phys. Rev. Lett.* **45**, 347.
- Bodin, H. A. B., 1984, in *Proceedings of the International Conference on Plasma Physics*, Lausanne, edited by M. Q. Tran and R. J. Verbeek (EEC, Brussels), Vol. I, p. 417.
- Bodin, H. A. B., and A. A. Newton, 1980, *Nucl. Fusion* **20**, 1255.
- Bondeson, A., G. Marklin, Z. G. An, H. H. Chen, Y. C. Lee, and C. S. Liu, 1981, *Phys. Fluids* **24**, 1682.
- Bruhns, H., C. Chin-Fatt, Y. P. Chong, A. W. DeSilva, G. C. Goldenbaum, H. R. Griem, G. W. Hart, R. A. Hess, J. H. Irby, and R. S. Shaw, 1983, *Phys. Fluids* **26**, 1616.
- Bruhns, H., G. Raupp, K. Sobel, J. Steiger, and A. Weichelt, 1984, in *Proceedings of the 6th U.S. Symposium on Compact Toroid Research*, edited by M. Yamada and R. Ellis, Jr. (Princeton Plasma Physics Laboratory, Princeton, N.J.), p. 25.
- Butt, E. P., C. W. Gowers, A. Mohri, A. A. Newton, D. C. Robinson, A. J. L. Verhage, M. R. C. Watts, Li Yin-An, and H. A. B. Bodin, 1975, *Proceedings of the 7th European Conference on Controlled Fusion and Plasma Physics*, Lausanne (Centre de Recherches en Physique des Plasmas, Lausanne), Vol. I, p. 39.
- Caramana, E. J., R. A. Nebel, and D. D. Schnack, 1983, *Phys. Fluids* **26**, 1305.
- Chandrasekhar, S., and P. C. Kendall, 1957, *Astrophys. J.* **126**, 457.
- DiMarco, J. N., 1983, in *Mirror Based and Field Reversed Approaches to Magnetic Fusion*, proceedings of the International School of Plasma Physics Course, edited by R. F. Post, D. E. Baldwin, and D. D. Ryutov [International School of Plasma Physics, Varenna (Como), Italy], Vol. II, p. 681.
- Edenstrasse, J. W., and W. Schuurman, 1983, *Phys. Fluids* **26**, 500.
- Faber, V., A. B. White, and G. M. Wing, 1982, *J. Math. Phys.* **23**, 1524.
- Faber, V., A. B. White, and G. M. Wing, 1985, *Plasma Phys. Cont. Fusion* **27**, 509.
- Finn, J. M., W. M. Mannheimer, and E. Ott, 1981, *Phys. Fluids* **24**, 1336.
- Frisch, U., A. Pouquet, J. Léorat, and A. Mazure, 1975, *J. Fluid Mech.* **68**, 769.
- Furth, H., 1981, *J. Vac. Sci. Technol.* **18**, 1073.
- Furth, H., 1985, *Phys. Fluids* **28**, 1595.
- Furth, H., J. Killeen, and M. N. Rosenbluth, 1963, *Phys. Fluids* **6**, 459.
- Gibson, R. D., and K. Whiteman, 1968, *Plasma Phys.* **10**, 1101.
- Goldenbaum, G. C., 1982, *Phys. Scr.* **T2/2**, 359.
- Goldenbaum, G. C., J. H. Irby, Y. P. Chong, and G. W. Hart, 1980, *Phys. Rev. Lett.* **44**, 393.
- Hameiri, E., and J. H. Hammer, 1982, *Phys. Fluids* **25**, 1855.
- Hart, G. W., A. Janos, D. D. Meyerhofer, and M. Yamada, 1985, *Phys. Fluids* (in press).
- Hasegawa, A., 1985, *Adv. Phys.* **34**, 1.
- Heyvaerts, J., and E. R. Priest, 1984, *Astron. Astrophys.* **137**, 63.
- Janos, A., G. W. Hart, C. H. Nam, and M. Yamada, 1985b, *Phys. Fluids* **28**, 3667.
- Janos, A., G. W. Hart, and M. Yamada, 1985a, *Phys. Rev. Lett.* **55**, 2868.
- Jarboe, T. R., 1985a, *Comments Plasma Phys.* **9**, 161.
- Jarboe, T. R., 1985b, *Bull. Am. Phys. Soc.* **30**, 1408.
- Jarboe, T. R., Cris W. Barnes, I. Henins, H. W. Hoida, S. O. Knox, R. K. Linford, and A. R. Sherwood, 1984, *Phys. Fluids* **27**, 13.
- Jarboe, T. R., I. Henins, H. W. Hoida, R. K. Linford, J. Marshall, D. A. Platts, and A. R. Sherwood, 1980, *Phys. Rev. Lett.* **45**, 1264.
- Jarboe, T. R., I. Henins, A. R. Sherwood, Cris W. Barnes, and H. W. Hoida, 1983, *Phys. Rev. Lett.* **51**, 39.
- Jensen, T., and M. S. Chu, 1981, *J. Plasma Phys.* **25**, 459.

- Jensen, T., and M. S. Chu, 1983, in *Proceedings of the 5th Symposium on Physics and Technology of Compact Toroids*, edited by A. L. Hoffman and R. D. Milroy (Mathematical Sciences Northwest Inc.), pp. 174–177.
- Jensen, T., and M. S. Chu, 1984, *Phys. Fluids* **27**, 2881.
- Kadomtsev, B. B., 1975, *Fiz. Plazmy* **1**, 710 [*Sov. J. Plasma Phys.* **1**, 389 (1975)].
- Kadomtsev, B. B., 1977, *Plasma Physics and Controlled Nuclear Fusion Research 1976, Proceedings of the 6th International Conference, Berchtesgaden, 1976* (IAEA, Vienna), Vol. I, p. 555.
- Katsurai *et al.*, 1984, *Proceedings of the 6th US-Japan Compact Toroid Symposium* (Hiroshima University, Hiroshima, Japan).
- Kawai, K., and A. A. Pietrzyk, 1981, *Bull. Am. Phys. Soc.* **26**, 905.
- Kondoh, Y., 1981, *Nucl. Fusion* **21**, 1607.
- Konigl, A., and A. R. Choudhuri, 1985, *Astrophys. J.* **289**, 173.
- Krüger, J., 1976a, *J. Plasma Phys.* **15**, 15.
- Krüger, J., 1976b, *J. Plasma Phys.* **15**, 31.
- Kruskal, M. D., and R. M. Kulsrud, 1958, *Phys. Fluids* **1**, 265.
- La Haye, R. J., T. H. Jensen, P. S. C. Lee, R. W. Moore, and T. Ohkawa, 1986, *Nucl. Fusion* **26**, 255.
- La Haye, R. J., P. S. C. Lee, R. W. Moore, and T. Ohkawa, 1984, *Bull. Am. Phys. Soc.* **29**, 1331.
- Mannheimer, W., 1981, *Phys. Fluids* **24**, 986.
- Martin, T. J., and J. B. Taylor, 1974, "Helically Deformed States in Toroidal Pinches," Culham Laboratory report (unpublished).
- Mattheus, W. H., and D. C. Montgomery, 1980a, in *Proceedings of the Reverse Field Pinch Theory Workshop*, edited by H. R. Lewis and R. A. Gerwin (Los Alamos National Laboratory, Los Alamos, New Mexico), Session V, paper A-5.
- Mattheus, W. H., and D. C. Montgomery, 1980b, *Ann. N.Y. Acad. Sci.* **357**, 203.
- Moffatt, H. K., 1978, *Magnetic Field Generation in Electrically Conducting Fluids* (Cambridge University Press, Cambridge/London/New York).
- Montgomery, D., L. Turner, and G. Vahala, 1978, *Phys. Fluids* **21**, 757.
- Nagata, M., Y. Honda, K. Ikegami, M. Nishikawa, A. Ozaki, N. Satomi, T. Uyama, and K. Watanabe, 1985, *Plasma Physics and Controlled Nuclear Fusion Research, 1984, Proceedings of the 10th International Conference, London, 1984* (IAEA, Vienna), Vol. II, p. 655.
- Newton, A. A., 1985, private communication.
- Nogi, Y., H. Ogura, Y. Osanai, K. Saito, S. Shiina, and H. Yoshimura, 1980, *J. Phys. Soc. Jpn.* **49**, 710.
- Ohkawa, T., M. Chu, C. Chu, and M. Schaffer, 1980, *Nucl. Fusion* **20**, 1464.
- Ortolani, S., 1984, in *Twenty Years of Plasma Physics, Proceedings of the ICTP Trieste Meeting*, edited by B. McNamara (World Scientific, Philadelphia/Singapore), p. 75.
- Ortolani, S., and G. Rostagni, 1983, *Nucl. Instrum. Methods* **207**, 35.
- Parker, E. N., 1957, *J. Geophys. Res.* **62**, 509.
- Petschek, H. E., 1965, in *AAS-NASA Symposium on the Physics of Solar Flares*, edited by W. N. Hess (NASA, Washington, D.C.), NASA SP-50, p. 425.
- Platts, D. A., J. C. Fernandez, T. R. Jarboe, and B. L. Wright, 1985, *Bull. Am. Phys. Soc.* **30**, 1454.
- Reiman, A., 1980, *Phys. Fluids* **23**, 230.
- Reiman, A., 1981, *Phys. Fluids* **24**, 956.
- Riyopoulos, S., A. Bondeson, and D. Montgomery, 1982, *Phys. Fluids* **25**, 107.
- Rosenbluth, M. N., and M. N. Bussac, 1979, *Nucl. Fusion* **19**, 489.
- Rusbridge, M. G., 1977, *Plasma Phys.* **19**, 499.
- Rusbridge, M. G., 1982, *Nucl. Fusion* **22**, 1291.
- Sato, T., and K. Kusano, 1985, *Plasma Physics and Controlled Nuclear Fusion Research 1984, Proceedings of the 10th International Conference, London, 1984* (IAEA, Vienna), Vol. II, p. 461.
- Schmidt, G., 1966, *Physics of High Temperature Plasmas* (Academic, New York).
- Sweet, P. A., 1958, in *Electromagnetic Phenomena in Cosmical Physics*, IAU Symposium No. 6, edited by B. Lehnert (Cambridge University Press, Cambridge), p. 123.
- Sykes, A., and J. A. Wesson, 1977, *Proceedings of the 8th European Conference on Controlled Fusion and Plasma Physics, Prague* (Czechoslovak Academy of Sciences, Prague), Vol. 1, p. 80.
- Tamano, T., T. Carlstrom, C. Chu, R. Goforth, G. Jackson, R. La Haye, T. Ohkawa, M. Schaffer, and P. Taylor, 1983, in *Mirror Based and Field Reversed Approaches to Magnetic Fusion*, proceedings of the International School of Plasma Physics Course, edited by R. F. Post, D. E. Baldwin, and D. D. Ryutov [International School of Plasma Physics, Varenna (Como), Italy], Vol. II, p. 653.
- Tamaru, T., K. Sugisaki, K. Hayase, T. Shimada, Y. Hirano, Y. Maejima, K. Ogawa, K. Hirano, S. Kitagawa, K. Sato, M. Wakatani, S. Yamada, H. Arimoto, Y. Kita, S. Yamaguchi, A. Nagata, S. Ido, and I. Kawakami, 1979, *Plasma Physics and Controlled Nuclear Fusion Research, 1978, Proceedings of the 7th International Conference, Innsbruck, 1978* (IAEA, Vienna), Vol. II, pp. 55–68.
- Taylor, J. B., 1974a, *Phys. Rev. Lett.* **33**, 1139.
- Taylor, J. B., 1974b, unpublished.
- Taylor, J. B., 1975, *Plasma Physics and Controlled Nuclear Fusion Research, 1974, Proceedings of the 5th International Conference, Tokyo, 1974* (IAEA, Vienna), Vol. I, p. 161.
- Taylor, J. B., 1976, in *Pulsed High Beta Plasmas, Proceedings of the Third Topical Conference, Abingdon, 1975*, edited by D. E. Evans (Pergamon, Oxford/New York), p. 59.
- Taylor, J. B., 1980, in *Proceedings of the Reverse Field Pinch Theory Workshop*, edited by H. R. Lewis and R. A. Gerwin (Los Alamos National Laboratory, Los Alamos, New Mexico), Session V, paper A-1.
- Taylor, J. B., and M. F. Turner, 1985, unpublished.
- Ting, A. C., W. H. Matthews, and D. Montgomery, 1986, *Phys. Fluids* (in press).
- Toyama, H., N. Asakura, K. Hattori, N. Inoue, S. Ishida, S. Matsuzuka, K. Miyamoto, J. Morikawa, Y. Nagayama, H. Nihei, S. Shinohara, Y. Ueda, K. Yamagishi, and Z. Yoshida, 1985, in *Proceedings of the 12th European Conference on Controlled Fusion and Plasma Physics, Budapest*, edited by L. Pocs and A. Montvai (European Physical Society, Geneva), Vol. I, p. 602.
- Turner, L., 1983, *Ann. Phys. (N.Y.)* **149**, 58.
- Turner, L., 1984, *Phys. Fluids* **27**, 1677.
- Turner, L., and J. P. Christiansen, 1981, *Phys. Fluids* **24**, 893.
- Turner, W. C., G. C. Goldenbaum, E. H. A. Granneman, J. H. Hammer, C. W. Hartman, D. S. Prono, and J. Taska, 1983, *Phys. Fluids* **26**, 1965.
- Turner, W. C., E. H. A. Granneman, C. W. Hartman, D. S. Prono, J. Taska, and A. C. Smith, Jr., 1981, *J. Appl. Phys.* **52**, 175.
- Vasyliunas, V. M., 1975, *Rev. Geophys. Space Phys.* **13**, 303.
- Verhage, A. J. L., A. S. Furzer, and D. C. Robinson, 1978,

- Nucl. Fusion **18**, 457.
- Voslamber, D., and D. K. Callebaut, 1962, Phys. Rev. **128**, 2016.
- Watt, R. G., and R. A. Nebel, 1983, Phys. Fluids **26**, 1168.
- Watt, R. G., J. A. Phillips, and A. A. Newton, 1985, private communication.
- Wells, D. R., and J. Norwood, 1969, J. Plasma Phys. **3**, 21.
- White, R. B., 1983, *Handbook of Plasma Physics* (North-Holland, Amsterdam).
- Whiteman, K., 1962, Plasma Phys. **7**, 293.
- Woltjer, L., 1958, Proc. Natl. Acad. Sci. U.S.A. **44**, 489.
- Wright, B. L., J. C. Fernandez, T. R. Jarboe, and D. A. Platts, 1985, Bull. Am. Phys. Soc. **30**, 1454.
- Yamada, M., R. Ellis, Jr., H. P. Furth, G. Hart, A. Janos, S. Jardin, F. Levinton, D. Meyerhofer, M. Mimura, C. H. Nam, S. Paul, A. Sperduti, S. Von Goeler, F. Wysocki, and P. Young, 1985, *Plasma Physics and Controlled Nuclear Fusion Research, 1984, Proceedings of the 10th International Conference, London, 1984* (IAEA, Vienna), Vol. 2., p. 535.
- Yamada, M., H. P. Furth, W. Hsu, A. Janos, S. Jardin, M. Okabayashi, J. Sennis, T. H. Stix, and K. Yamazaki, 1981, Phys. Rev. Lett. **46**, 188.